Supporting Information

A Light-Gated Molecular Shuttle With Catalyzing, Reacting and Regulatory Functions

Nazar Rad, and Volodymyr Sashuk*

Institute of Physical Chemistry, Polish Academy of Sciences, Kasprzaka 44/52, 01-224 Warsaw, Poland

vsashuk@ichf.edu.pl

Contents

1. General information

All chemicals were purchased as reagent grade from commercial suppliers (Sigma-Aldrich, AlfaAesar) and used without further purification. The solvents used (Merck, ChemPur, PoCh) were of analytical grade quality. Deuterated solvents were purchased from Armar Chemicals. Experiments were performed at room temperature unless otherwise noted. The progress of organic reactions was monitored by thin layer chromatography (TLC) using Merck silica gel 60 F254 (0.2 mm) on alumina plates. The products were purified by column chromatography (CC) using Merck silica gel 60 (230-400 mesh ASTM). NMR spectra were recorded on Bruker 400 and 600 MHz instruments. The chemical shifts (δ) are given in ppm relative to TMS, coupling constants are (J) in Hz. High-resolution ESI mass spectra were recorded on a SYNAPT spectrometer. UV-Vis spectra were taken on a Evolution220 spectrophotometer from Thermo Scientific. UV-Vis samples were irradiated using Epistar 3W 365 and 430 m light-emitting diodes (LED) mounted directly over a cuvette at a distance of 1 cm. NMR samples were illuminated via an optical fiber immersed into solution and connected with Prizmatix mic-LED (445 nm). The pH was measured using HI 3220 pH Meter equipped with InLab® Micro glass electrode (Mettler Toledo) and converted to pD values by adding 0.4 units [P. K. Glasoe et al. *J. Phys. Chem.* **1960**, *64*, 188]. Isothermal titration calorimetry (ITC)

experiments were carried out on a Malvern MicroCal PEAQ-ITC at 25°C in deionized water. Deionized water (18.2 MΩ·cm) was obtained from the Milli-Q station.

2. Synthesis

*Synthesis of **2***: Compound **1** was synthesized following the procedure described previously [P. K. Kundu et al. *Nanoscale* **2016**, *8*, 19280]. **1** (6g, 14.9 mmol) was dissolved in 56 mL of water. 1.83 g of Na_2CO_3 (17.3 mmol) was dissolved in 34 mL of water. Prepared sodium carbonate solution was dropped into the solution of **1** under stirring for 15 min. The reaction was continued to stir for 15 min. The product was extracted with Et_2O (3x20 mL). The extracts were dried with $MgSO_4$ and concentrated under reduced pressure. The residue was purified by column chromatography (Et_2O/hexane= 1:9) to give **2** as a pale violet liquid (4g, 76%). **^{1}H NMR** (400 MHz, $CDCl_3$) δ 7.16-7.05 (m, 2H), 6.76 (t, J = 7.4 Hz, 1H), 6.53 (d, J = 7.8 Hz, 1H), 3.85 (d, J = 12.2 Hz, 2H), 3,49 (t, J = 7.6 Hz, 2H), 3.45-3.35 (m, 3H), 1.91-1.79 (m, 3H), 1.70-1.59 (m, 2H), 1.51-1.39 (m, 4H), 1.34 (s, 6H). **^{13}C NMR** (101 MHz, $CDCl_3$) δ 161.65, 145.97, 137.55, 127.46, 121.80, 118.16, 105.01, 72.84, 44.17, 42.21, 33.88, 32.71, 30.06, 28.62, 28.08, 27.95, 27.05, 26.01. **HRMS (ESI) m/z**: calcd for $C_{18}H_{27}NBr$: 336.1327 $[M+H]^+$; found: 336.1327.

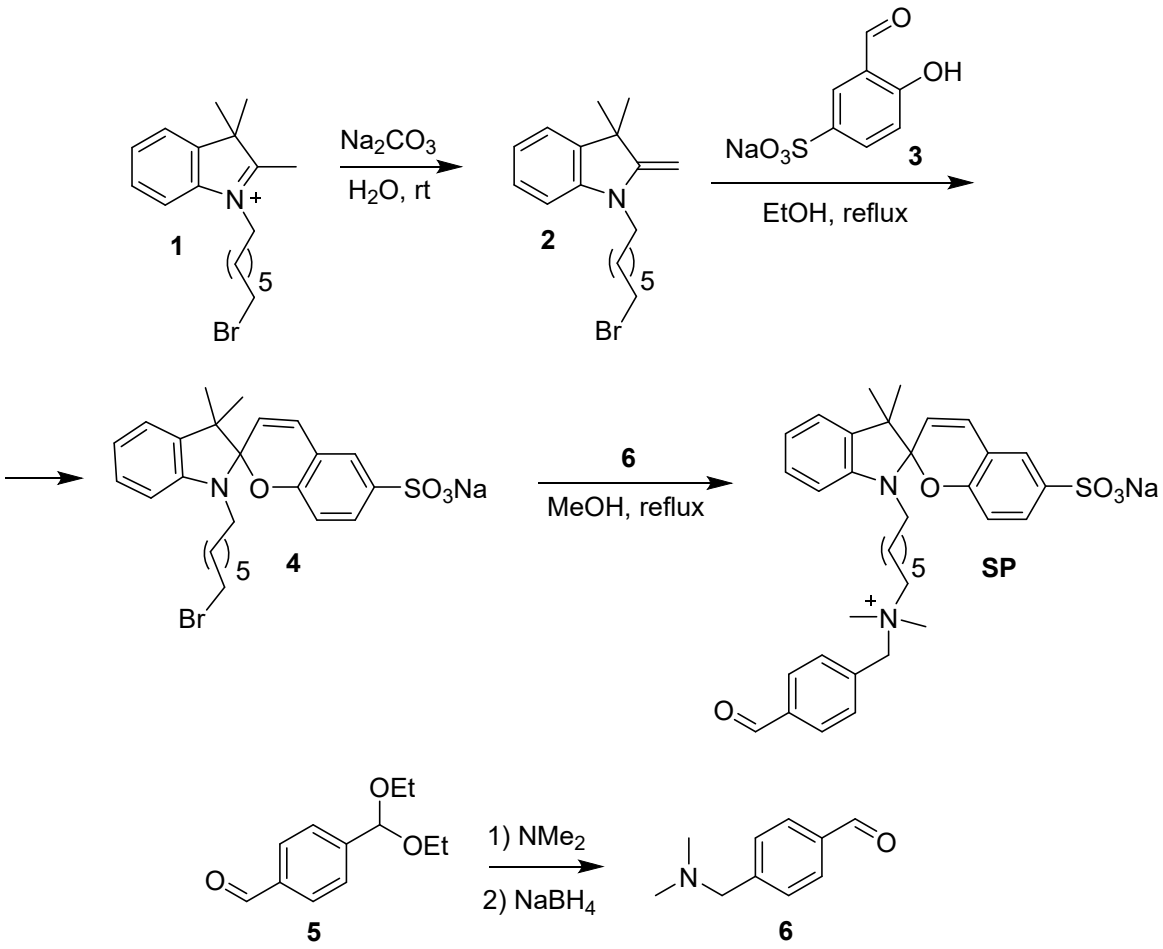

Figure S1. Synthesis of the axle.

*Synthesis of **4**.* Compound **3** was synthesised following the procedure described previously [C. Li et al. *J. Am. Chem. Soc.* **2020**, *142*, 8447]. The mixture of **2** (1.75 g, 5.2 mmol) and **3** (1.22 g, 5.46 mmol) was refluxed in 80 mL of ethanol under argon for 20 h. The solution was concentrated under reduced pressure. The residue was purified by column chromatography (DCM/MeOH = 8:2) to give **4** as an orange solid (2.17 g, 71%). **^{1}H NMR** (400 MHz, DMSO-d_6) δ 7.43 (d, J = 2.1 Hz, 1H), 7.32 (dd, J = 8.3, 2.1, 1H), 7.11-6.98 (m, 3H), 6.73 (t, J = 7.4 Hz, 1H), 6.60-6.47 (m, 2H), 5.76 (d, J = 10.2 Hz, 1H), 3.49 (t, J = 6.7 Hz, 2H), 3.17-2.98 (m, 2H), 1.80-1.68 (m, 2H), 1.64-1.39 (m, 2H), 1.38-1.20 (m, 6H), 1.19 (s, 3H), 1.08 (s, 3H). **^{13}C NMR** (101 MHz, DMSO-d_6) δ 154.23, 147.59, 140.94, 136.44, 129.54, 127.84, 127.69, 124.90, 121.99, 120.25, 118.82, 117.76, 113.88, 106.55, 104.93, 52.17, 43.37, 35.68, 32.61, 28.81, 28.34, 27.88, 26.92, 26.29, 20.13. **HRMS (ESI) m/z**: calcd for $C_{25}H_{29}NO_4SBr$: 518.0982 $[M]^-$; found: 518.1001.

*Synthesis of **6**.* Compound **5** was synthesized following the procedure described previously [N. Rad et al. *Angew. Chem. Int. Ed.* **2019**, *58*, 11340]. To a solution of **5** (2.91 g, 14 mmol)

in 85 mL of MeOH, 33% aq. solution of $HNMe_2$ (5 mL, 28 mmol) was added. The mixture was stirred overnight, then cooled to 0°C, and $NaBH_4$ (0.80 g, 21 mmol) was added portionwise for 15 min. The cooling bath was removed, and the reaction mixture was stirred for 5 h. The mixture was quenched with 50 mL of water and extracted with EtOAc (3x30 mL). The extracts were dried with Na_2SO_4, filtered, and concentrated under reduced pressure. The residue was dissolved in 10 mL of MeOH, and 50 mL of 1 M HCl was added. The solution was stirred for 1 h. The solvent was evaporated, and the residue was dissolved in water. The pH of the solution was adjusted with NaOH to the value 9-10. The product was extracted with Et_2O (3x30 mL). The extracts were dried with Na_2SO_4, filtered, and concentrated under reduced pressure. The residue was purified by column chromatography by elution with EtOAc /DCM/Et_3N (200:100:1.5) followed by EtOAc/Et_3N (300:1.5) to give **6** as a pale yellow liquid (1.68 g, 74%). **^{1}H NMR** (400 MHz, $CDCl_3$) δ 10.00 (s, 1H), 7.84 (d, J = 8.2 Hz, 2H), 7.49 (d, J = 7.9 Hz, 2H), 3.50 (s, 2H), 2.26 (s, 6H). **^{13}C NMR** (101 MHz, $CDCl_3$) δ 191.98, 146.33, 135.47, 129.78, 129.42, 64.03, 45.48. **HRMS (ESI) m/z**: calcd for $C_{10}H_{14}NO$: 164.1074 $[M]^+$; found: 164.1075.

*Synthesis of **SP**.* **4** (1.00 g, 1.85 mmol) was dissolved in 22 mL of MeOH under argon and **6** (0.603 g, 3.7 mmol) was added. The solution was refluxed for 44 h and concentrated under reduced pressure. The residue was purified by column chromatography. Elution with DCM/MeOH (9:1) followed by DCM/MeOH (8:2) gave the product as an orange solid (0.53 g, 42 %). **^{1}H NMR** (400 MHz, DMSO-d_6) δ 10.10 (s, 1H), 8.03 (d, J = 7.8 Hz, 2H), 7.80 (d, J = 7.8 Hz, 2H), 7.46 (d, J = 2.1 Hz, 1H), 7.36 (dd, J = 8.4 Hz, 2.2 Hz, 1H), 7.11-7.03 (m, 3H), 6.73 (t, J = 7.4 Hz, 1H), 6.57 (d, J = 8.4 Hz, 1H) 6.51 (d, J = 7.7 Hz, 1H), 5.76 (d, J = 10.2 Hz, 1H), 4.64 (s, 2H), 3.23-3.00 (m, 4H), 2.96 (s, 6H), 1.71-1.53 (m, 3H), 1.41-1.25(m, 3H), 1.23 (s, 3H), 1.19-1.13 (m, 2H), 1.08 (s, 3H), 1.05-0.95 (m, 2H). **^{13}C NMR** (101 MHz, DMSO-d_6) δ 193.45, 153.90, 147.01, 141.15, 137.50, 136.52, 134.81, 134.29, 130.10, 129.64, 127.85, 127.64, 124.88, 122.02, 119.79, 118.74, 117.74, 114.10, 106.55, 104.30, 65.77, 64.49, 51.90, 49.63, 42.77, 28.30, 27.57, 26.70, 26.56, 25.94, 22.32, 20.14. **HRMS (ESI) m/z**: calcd for $C_{35}H_{43}N_2O_5S$: 603.2913 $[M]^+$; found: 603.2893.

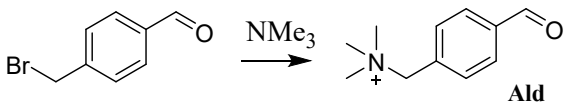

Ald

*Synthesis of **Ald**.* 4-(bromomethyl)benzaldehyde was synthesized following the procedure described previously [N. Rad et al. *Angew*. *Chem*. *Int*. *Ed*. **2019**, *58*, 11340]. To a solution of 4-(bromomethyl)benzaldehyde (298 mg, 1.5 mmol) in 5 mL of dry MeCN, 33 % ethanolic solution of NMe_3 (0.59 mL, 2.25 mmol) was added. The reaction mixture was stirred overnight and concentrated under reduced pressure. The residue was rinsed with Et_2O (3x10 mL) and dried to yield the product as a white solid (380 mg, 95%). **^{1}H NMR** (400 MHz, DMSO-d_6) δ 10.11 (s, 1H), 8.05 (d, J = 8.1 Hz, 2H), 7.80 (d, J = 7.9 Hz, 2H), 4.72 (s, 2H), 3.09 (s, 9H). **^{13}C NMR** (101 MHz, DMSO-d_6) δ 193.47, 137.57, 134.89, 134.12, 130.17, 67.30, 52.43. **HRMS (ESI) m/z**: calcd for $C_{11}H_{16}NO$: 178.1231 $[M]^+$; found: 178.1232.

Cucurbit[7]uril **CB7** was synthesized by following the previously described procedure [N. Rad et al. *Angew*. *Chem*. *Int*. *Ed*. **2019**, *58*, 11340].

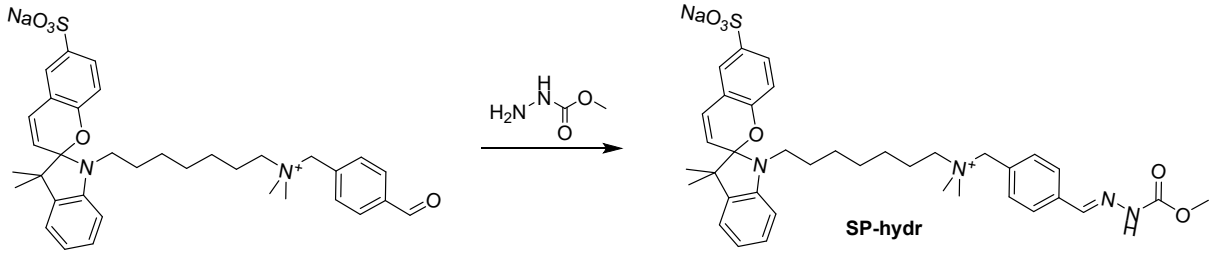

*Synthesis of **SP**-**hydr***. To a solution of **SP** (97 mg, 0.16 mmol) in 3 mL of MeOH, 15.8 mg (0.176 mmol) of methyl hydrazinocarboxylate was added. The reaction mixture was stirred for 16 h and then concentrated under reduced pressure. The residue was washed with Et_2O (2x10mL) and dried to give the product as an yellow powder (116 mg, 93 %). **^{1}H NMR** (400 MHz, DMSO-d_6) δ 11.25 (s, 1H), 8.09 (s, 1H), 7.74 (d, J = 7.8 Hz, 2H), 7.59 (d, J = 7.8 Hz, 2H), 7.47 (s, 1H), 7.35 (d, J = 7.6 Hz, 1H), 7.12-7.01 (m, 3H), 6.73 (t, J = 7.4 Hz, 1H), 6.57 (d, J = 8.4 Hz, 1H) 6.51 (d, J = 7.7 Hz, 1H), 5.76 (d, J = 10.2 Hz, 1H), 4.54 (s, 2H), 3.70 (s, 1H), 3.22-3.00 (m, 4H), 2.93 (s, 6H), 1.70-1.50 (m, 3H), 1.43-1.25 (m, 3H), 1.22 (s, 3H), 1.19-1.13 (m, 2H), 1.08 (s, 3H), 1.06-0.95 (m, 2H). **^{13}C NMR** (101 MHz, DMSO-d_6) δ 153.92, 147.07, 141.15, 136.51, 133.83, 129.66, 127.85, 127.64, 127.29, 124.88, 122.02, 119.83, 118.75, 117.74, 114.07, 106.55, 104.36, 66.12, 65.36, 64.08, 52.48, 51.93, 49.48, 42.82, 28.33, 27.68, 26.66, 26.60, 25.98, 22.28, 20.13, 15.62. **HRMS (ESI) m/z**: calcd for $C_{37}H_{46}N_4O_6NaS$: 397.3038 $[M+Na]^+$; found: 397.3036.

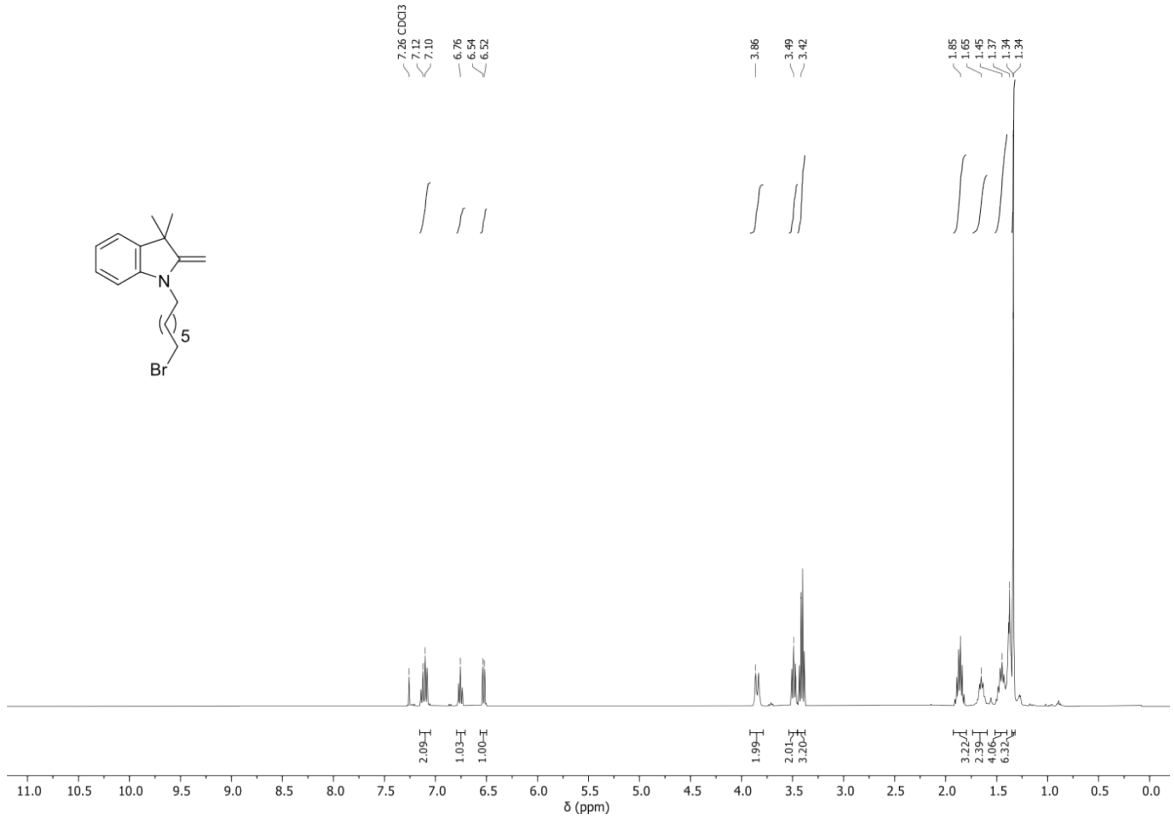

Figure S1. ^{1}H NMR spectrum of **2** in $CDCl_3$ (298 K).

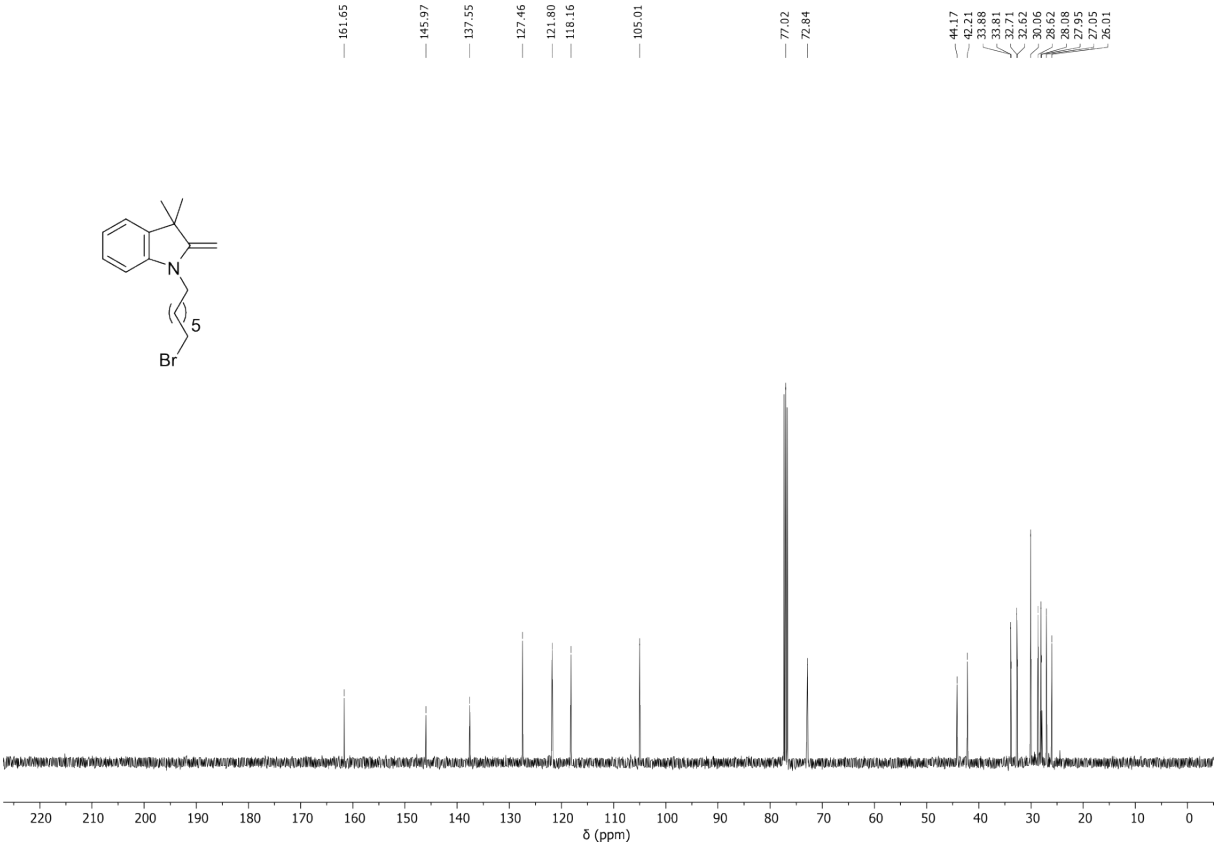

Figure S2. ^{13}C NMR spectrum of **2** in $CDCl_3$ (298 K).

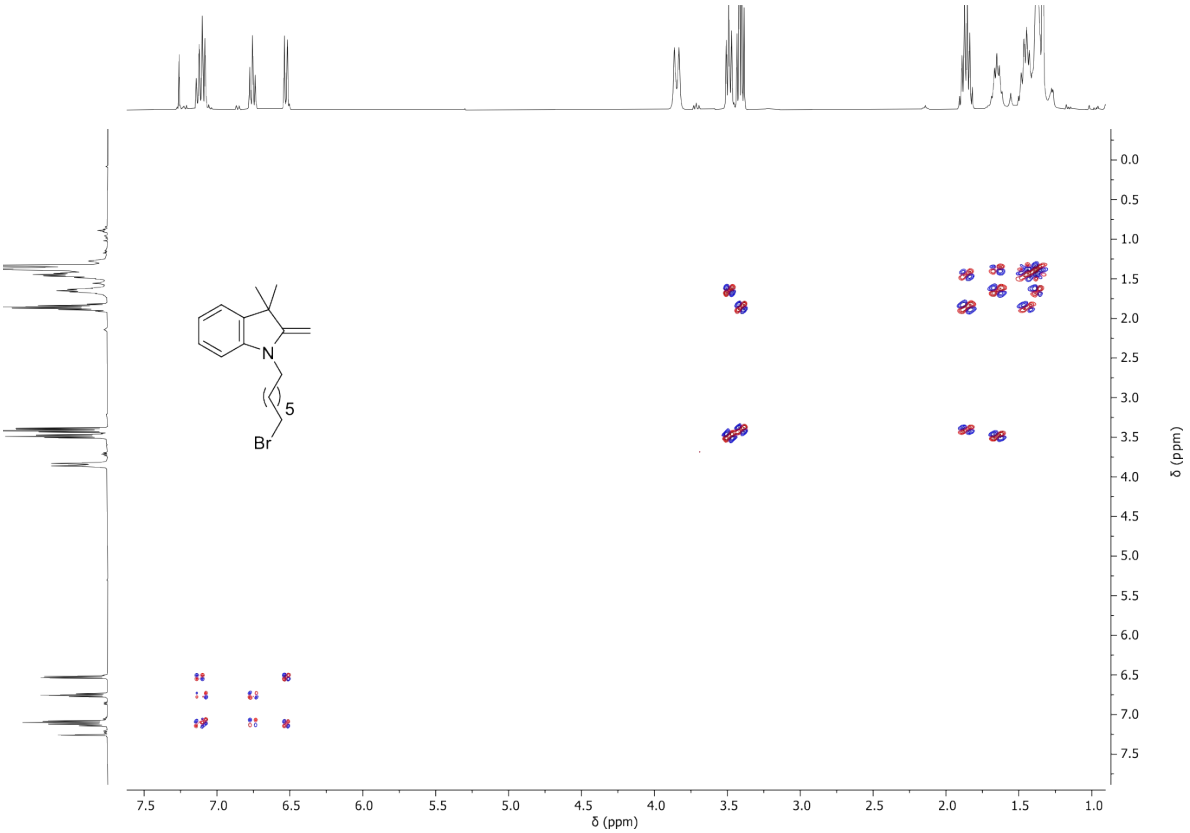

Figure S3. COSY spectrum of **2** in $CDCl_3$ (298 K).

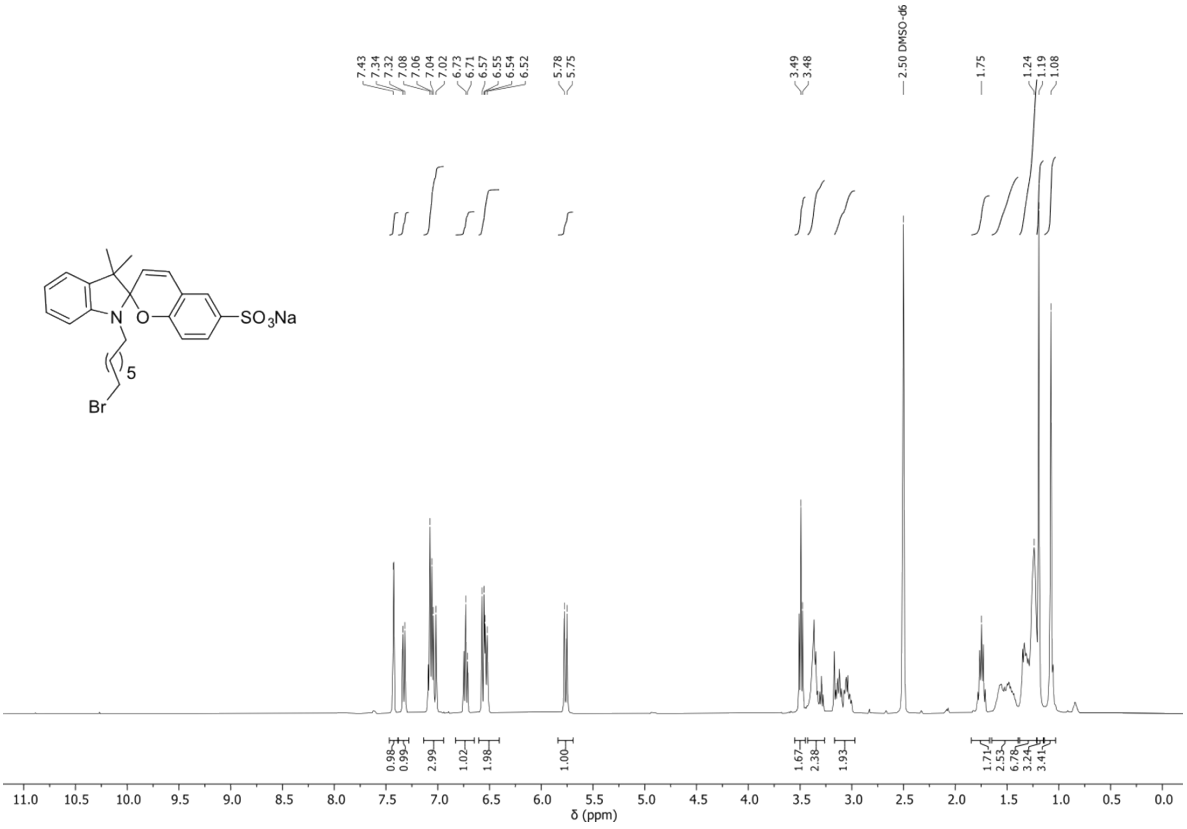

Figure S4. ^{1}H NMR spectrum of **4** in DMSO-d_6 (298 K).

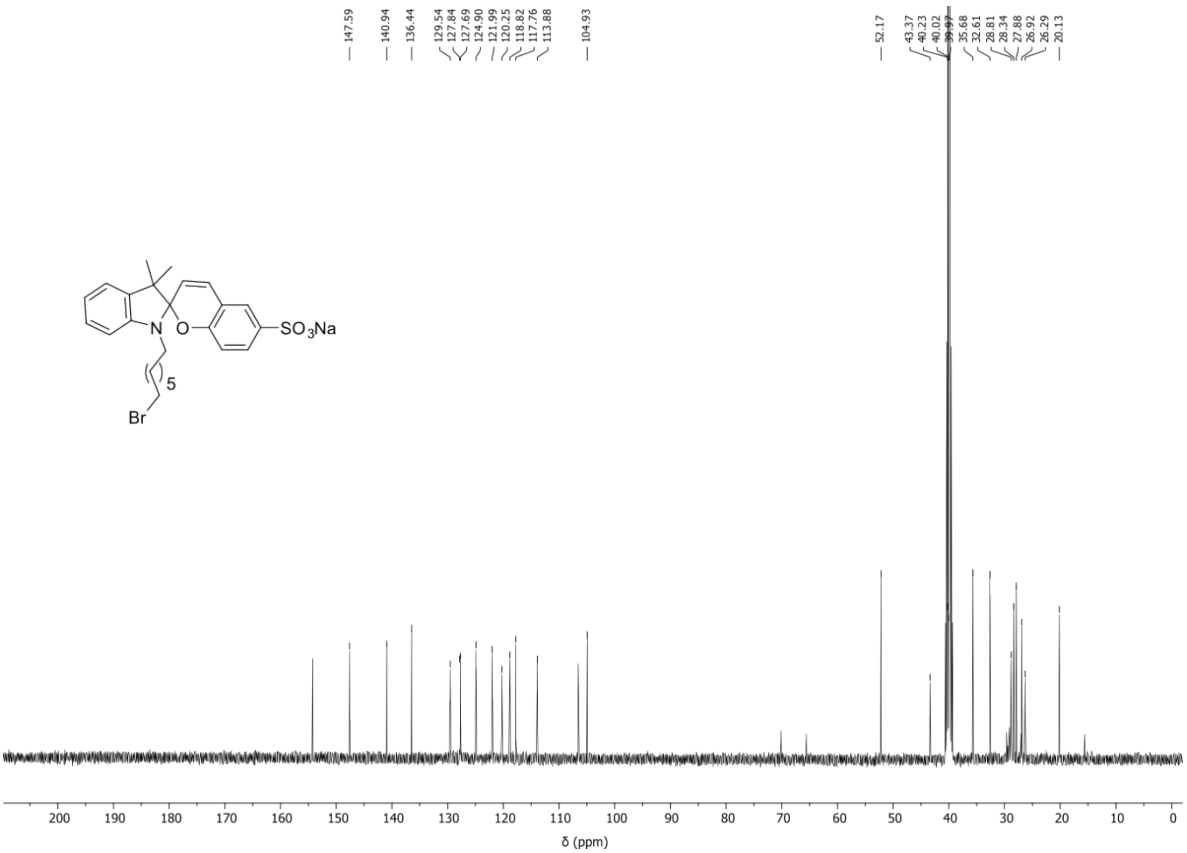

Figure S5. ^{13}C NMR spectrum of **4** in DMSO-d_6 (298 K).

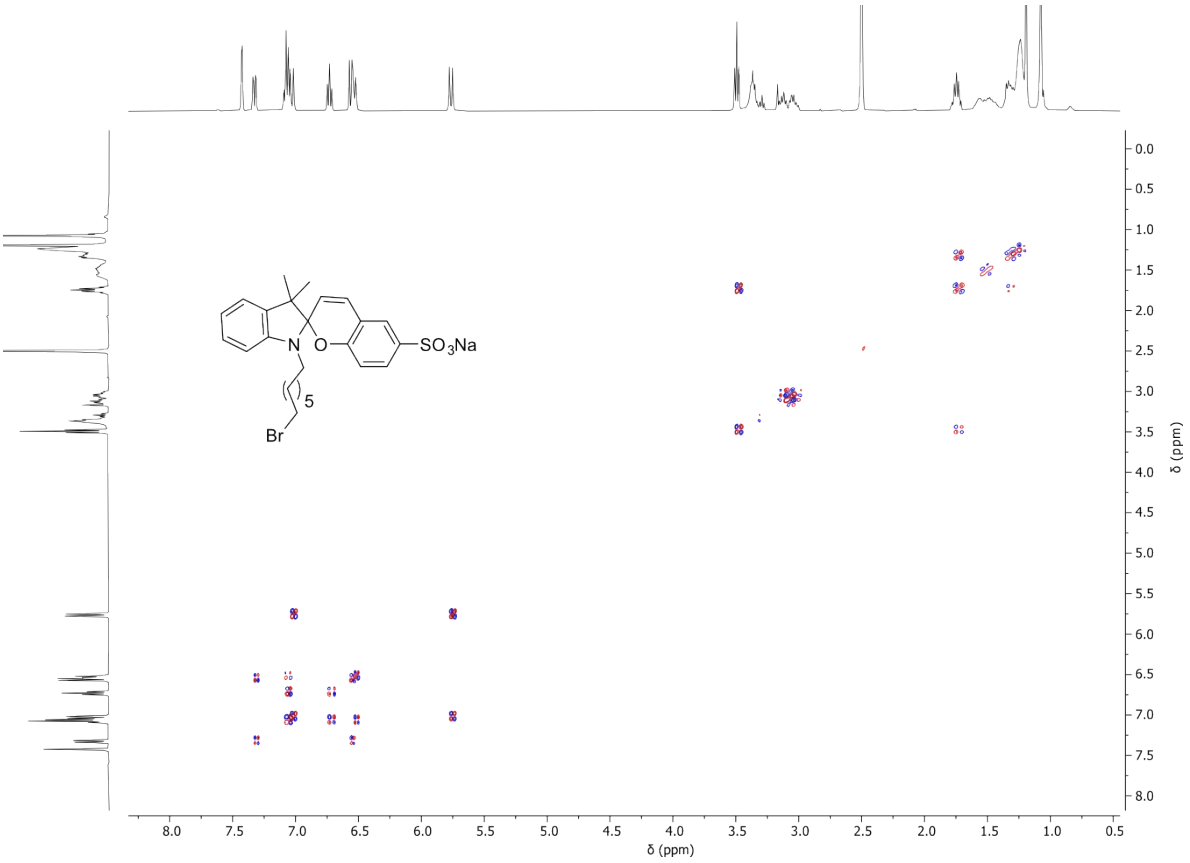

Figure S6. COSY spectrum of **4** in DMSO-d_6 (298 K).

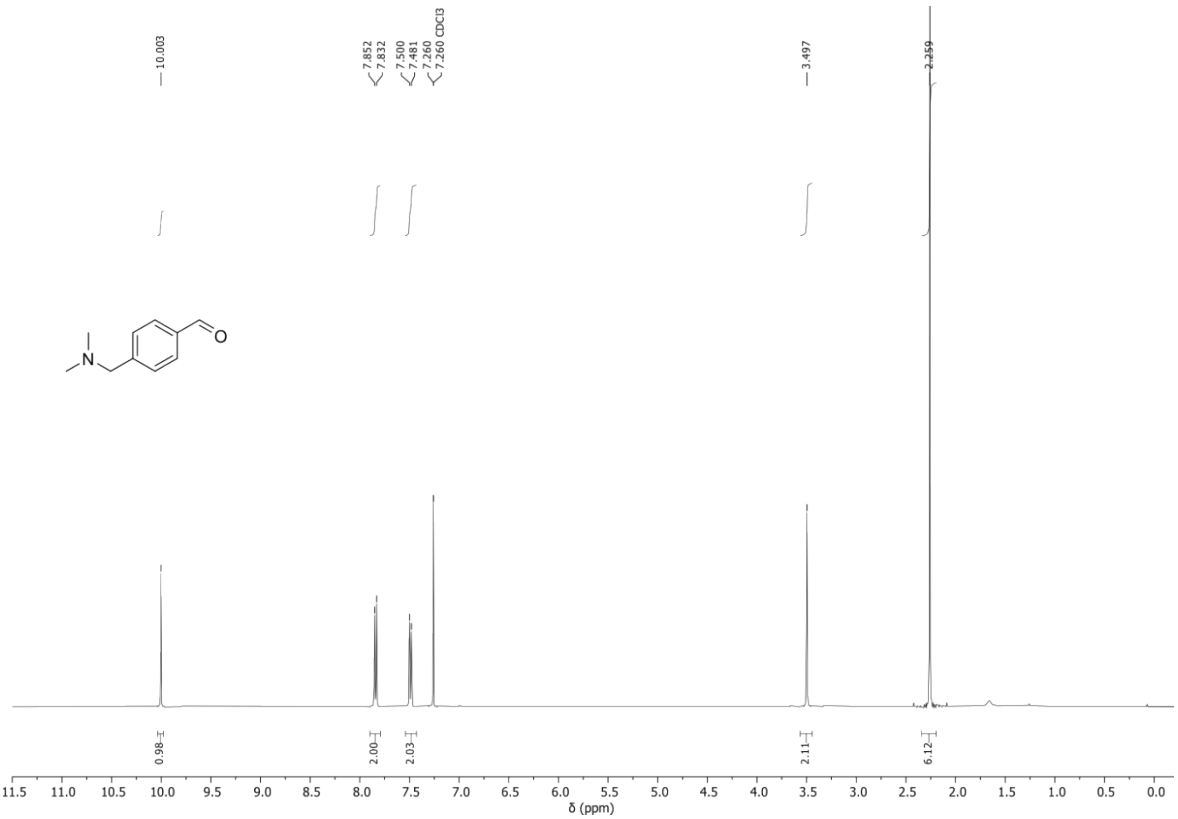

Figure S7. ^{1}H NMR spectrum of **6** in $CDCl_3$ (298 K).

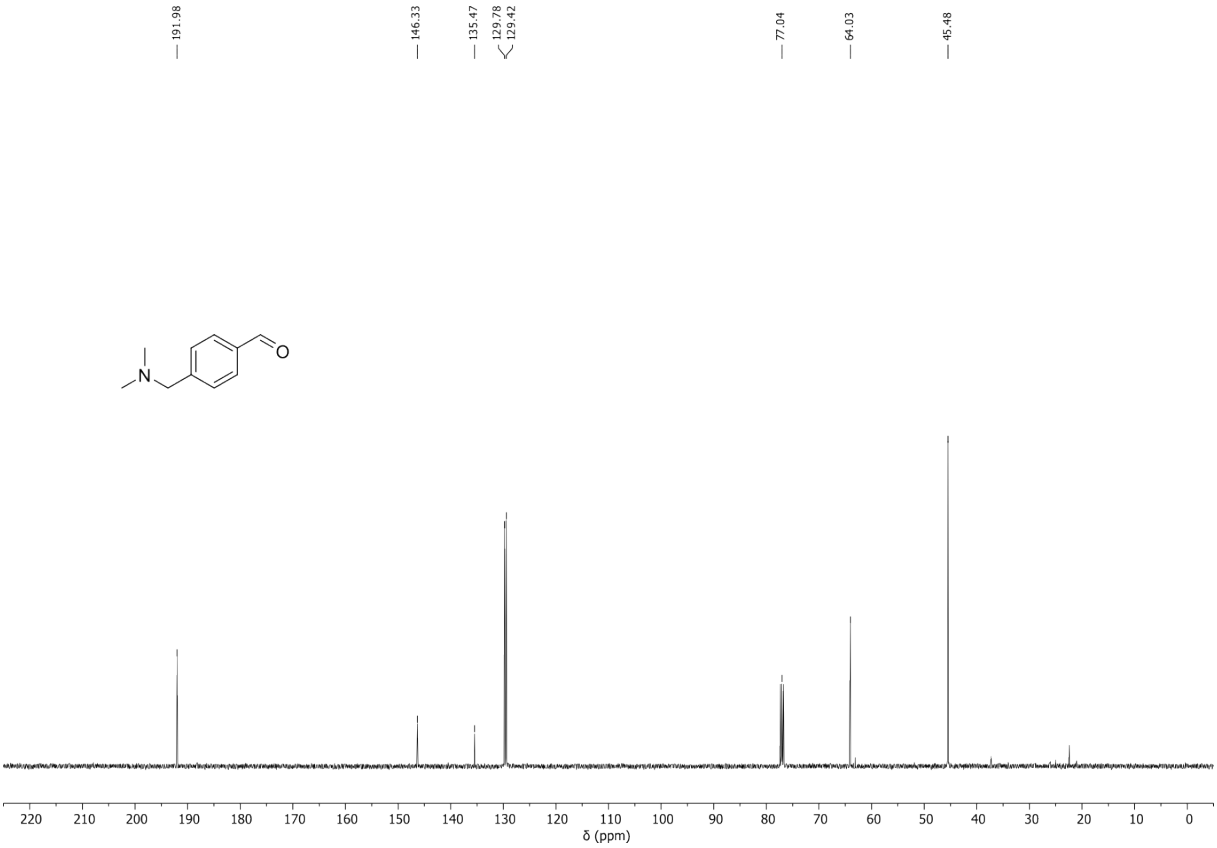

Figure S8. ^{13}C NMR spectrum of **6** in $CDCl_3$ (298 K).

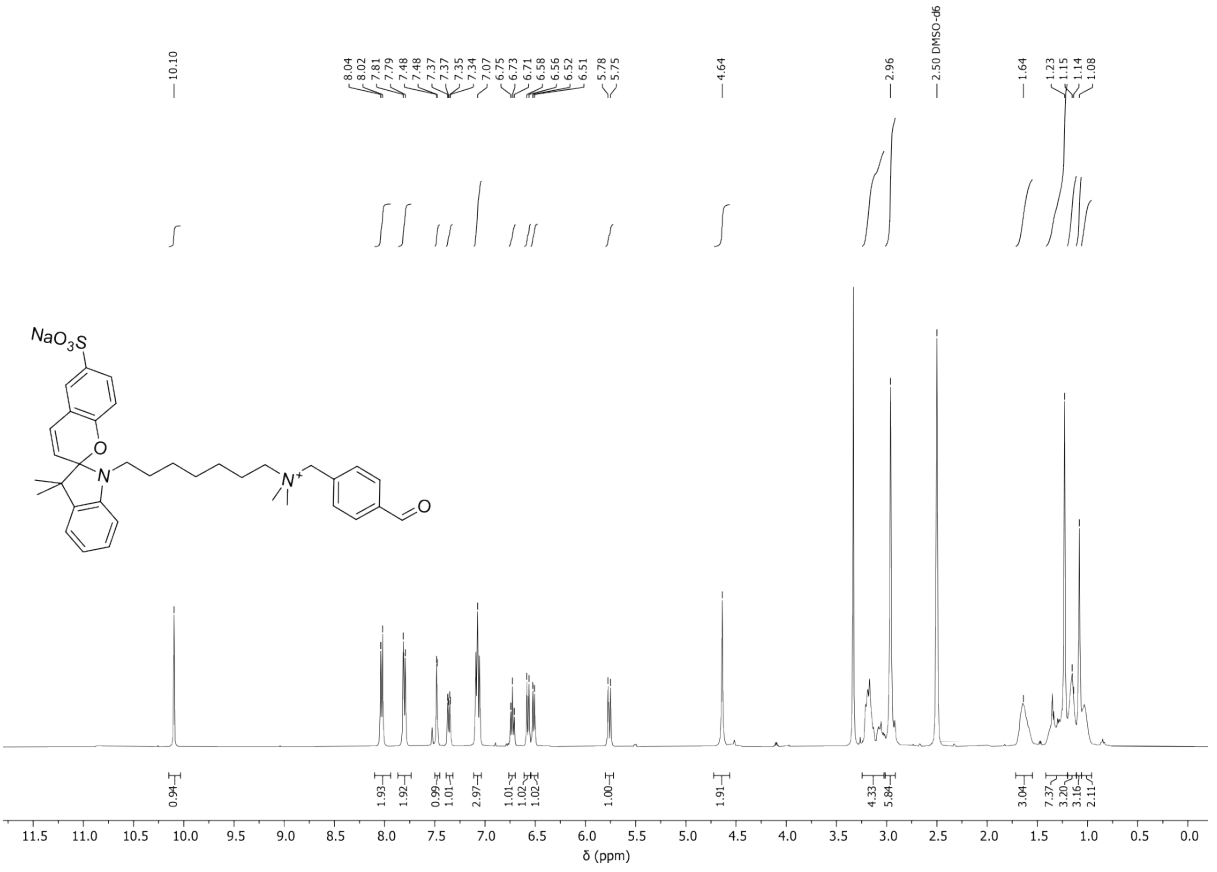

Figure S9.[1]H NMR spectrum of **SP** in DMSO-d_6 (298 K).

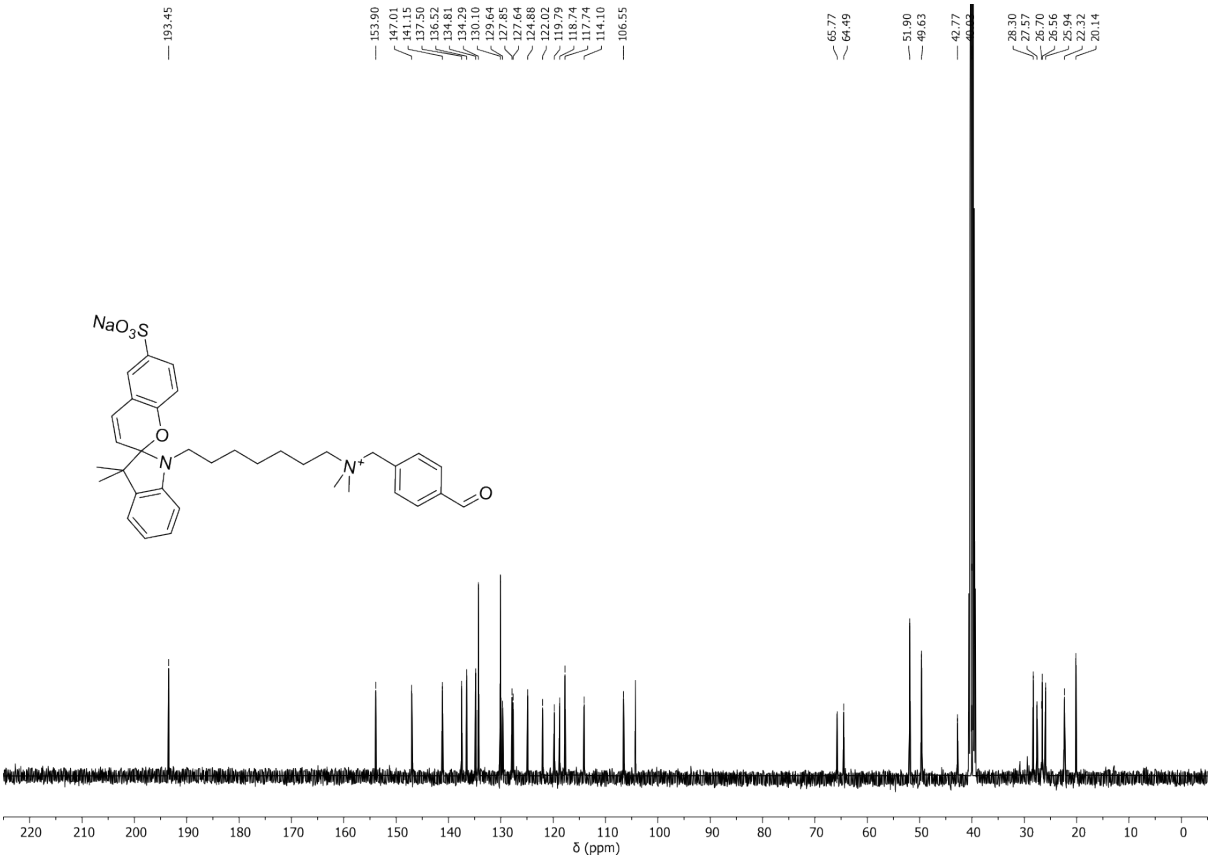

Figure S10. [13]C NMR spectrum of **SP** in DMSO-d_6 (298 K).

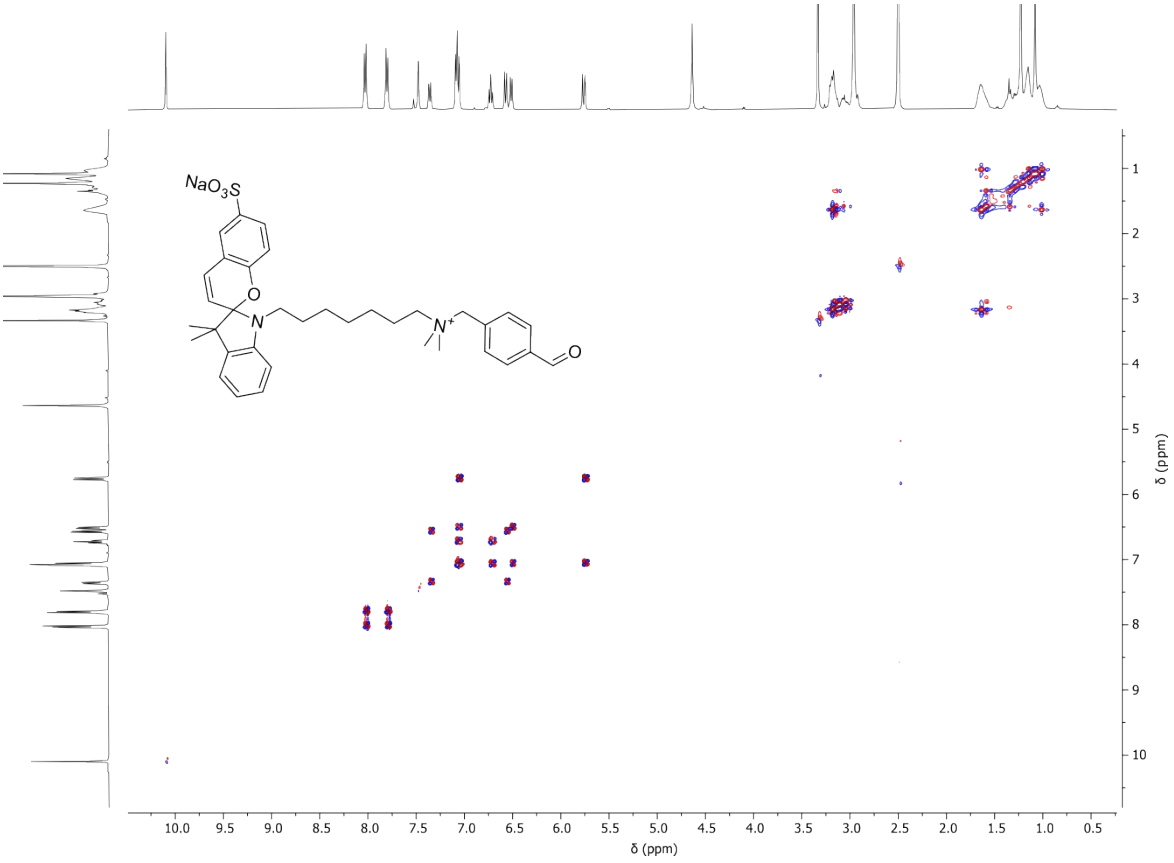

Figure S11. COSY spectrum of **SP** in DMSO-d_6 (298 K).

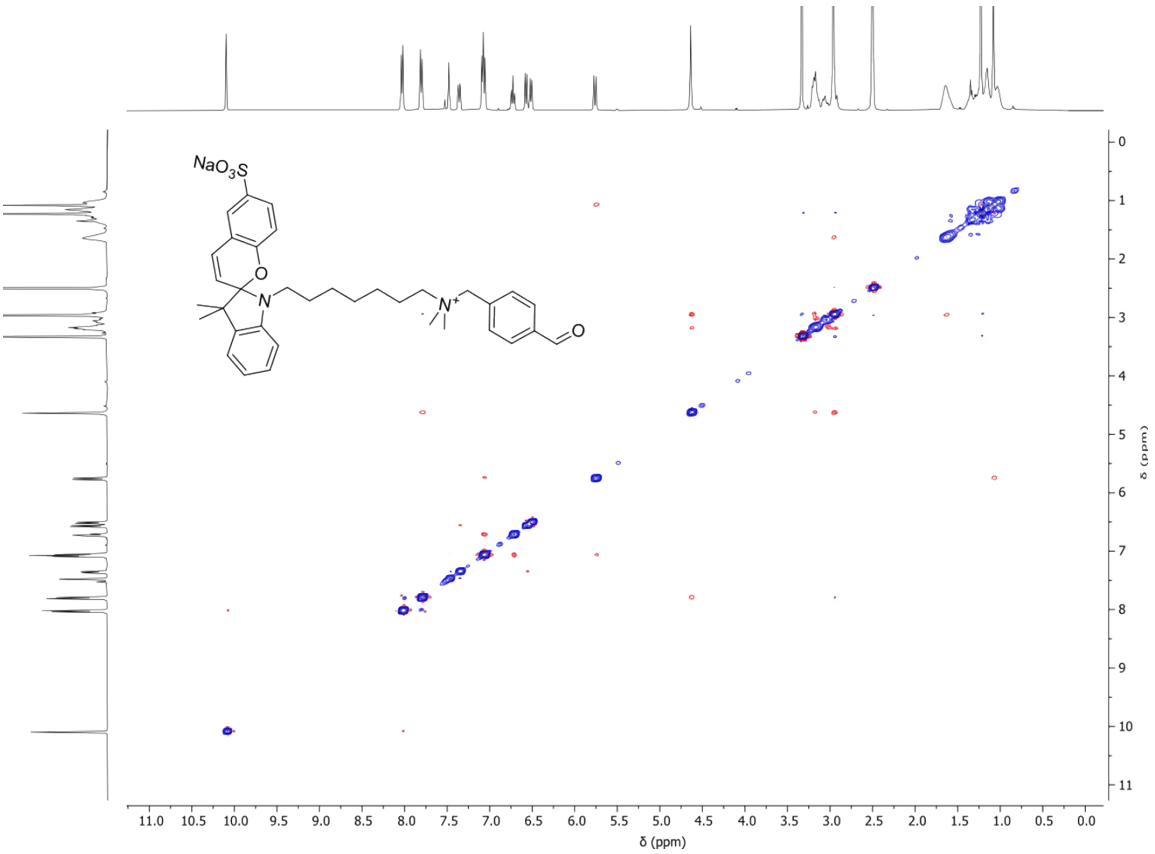

Figure S12. ROESY spectrum of **SP** in DMSO-d_6 (298 K).

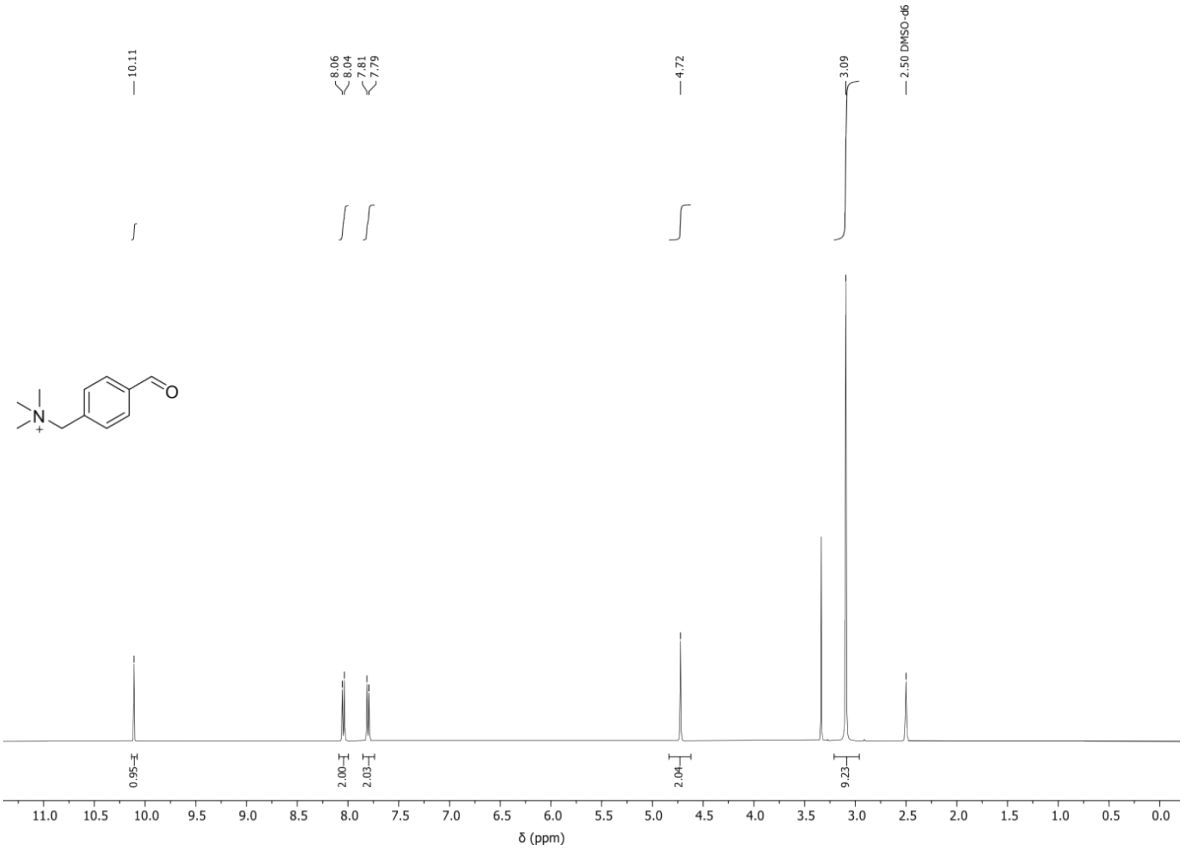

Figure S13. ^{1}H NMR spectrum of **Ald** in DMSO-d_6 (298 K).

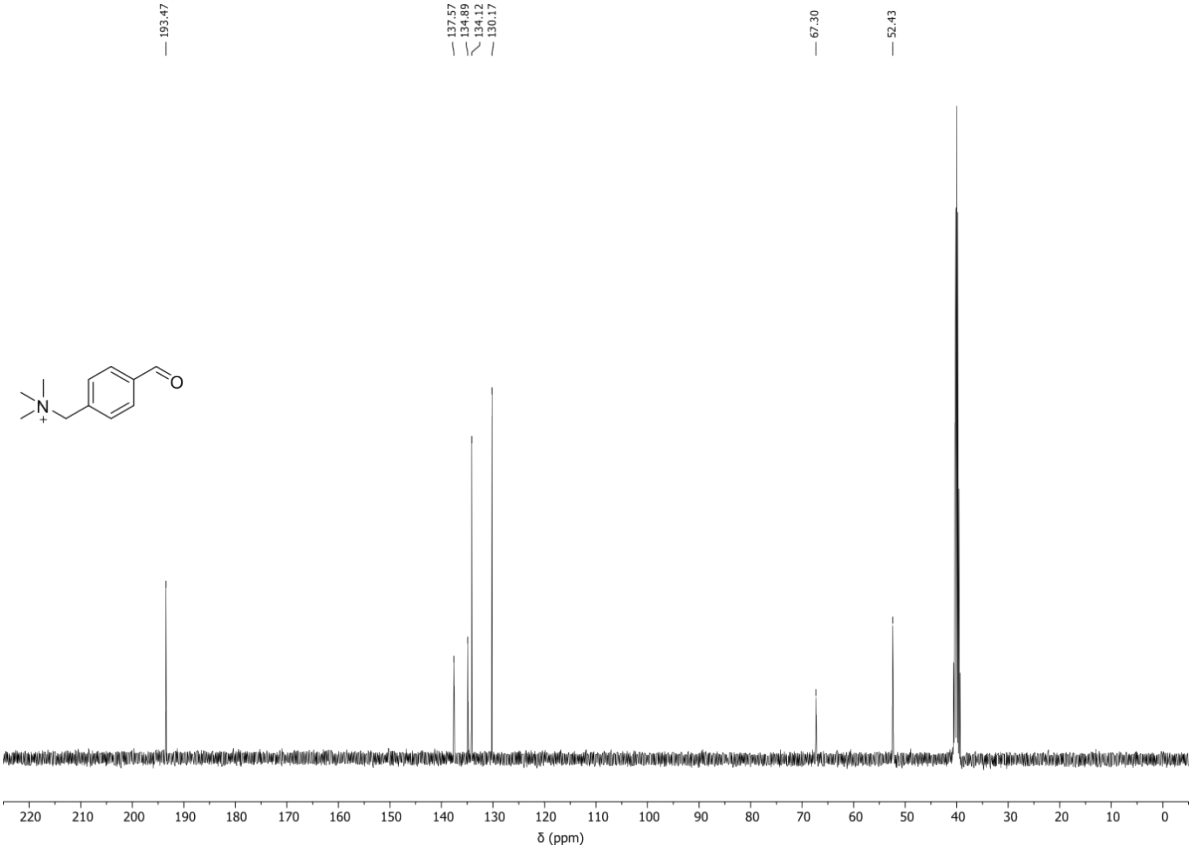

Figure S14. ^{13}C NMR spectrum of **Ald** in DMSO-d_6 (298 K).

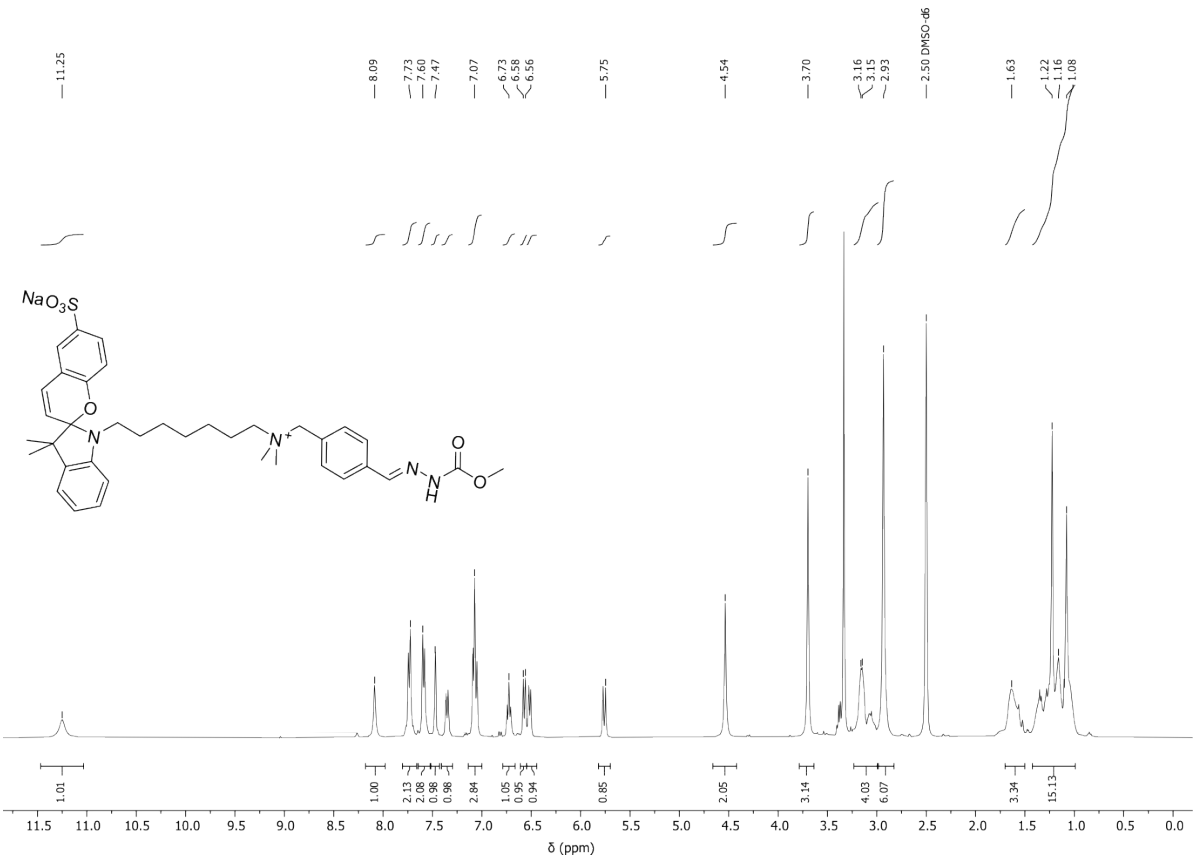

Figure S15. ^{1}H NMR spectrum of **SP-hydr** in DMSO-d_6 (298 K).

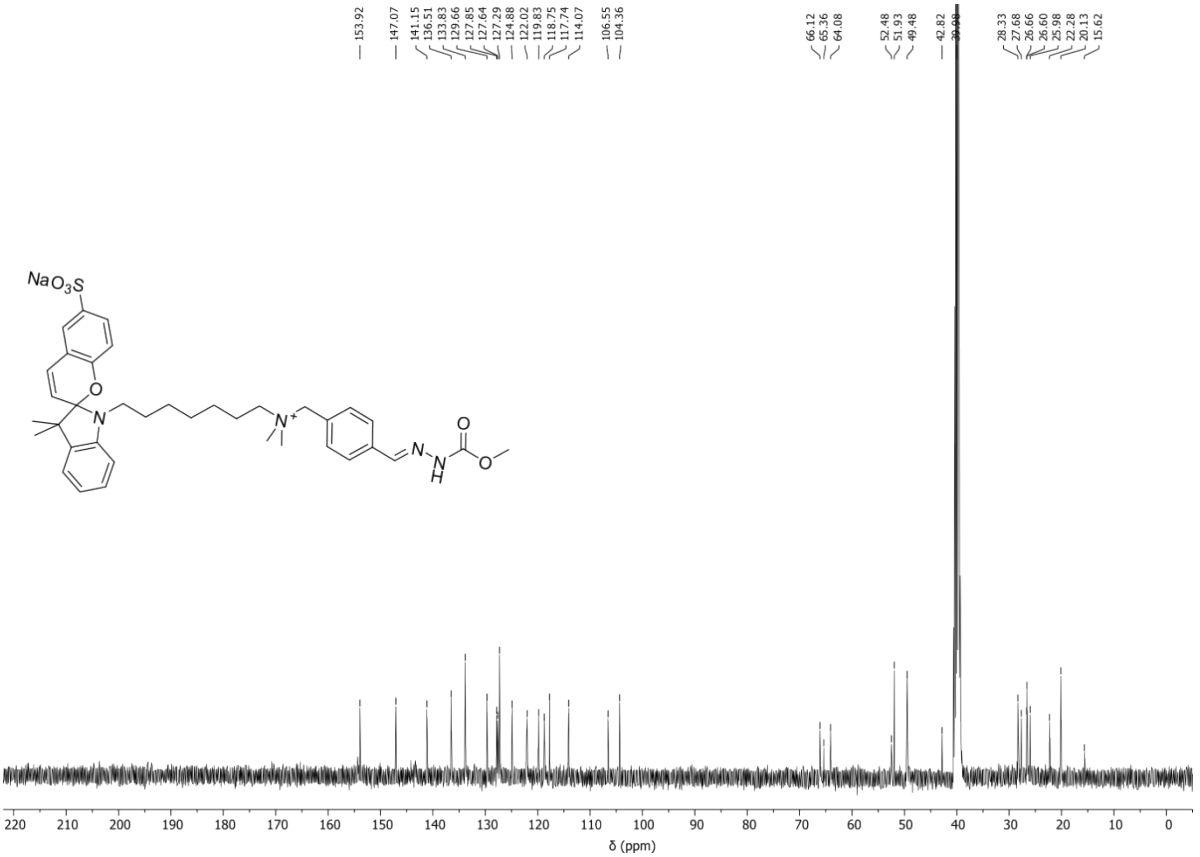

Figure S16. ^{13}C NMR spectrum of **SP-hydr** in DMSO-d_6 (298 K).

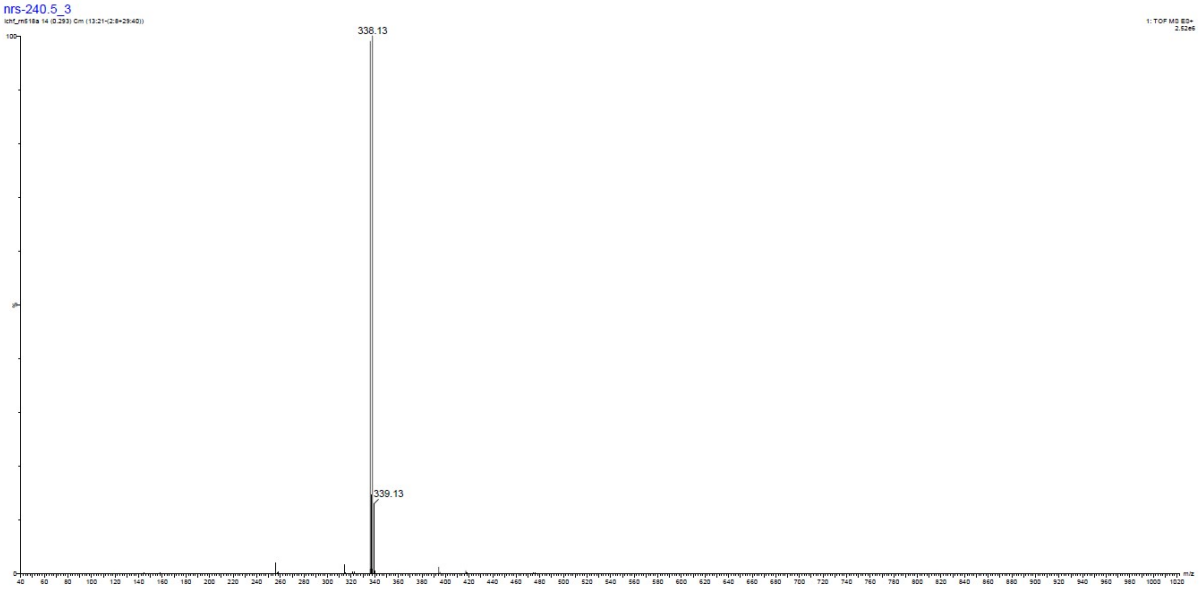

Figure S17. Mass spectrum of **2** under electrospray ionization in positive ion mode.

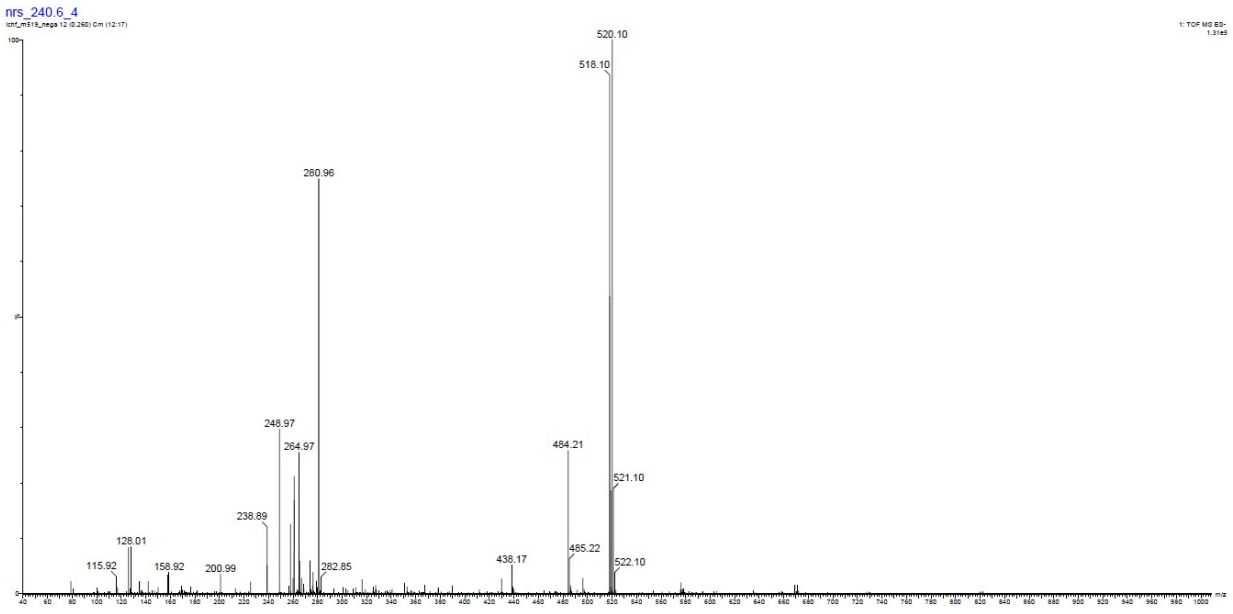

Figure S18. Mass spectrum of **4** under electrospray ionization in positive ion mode.

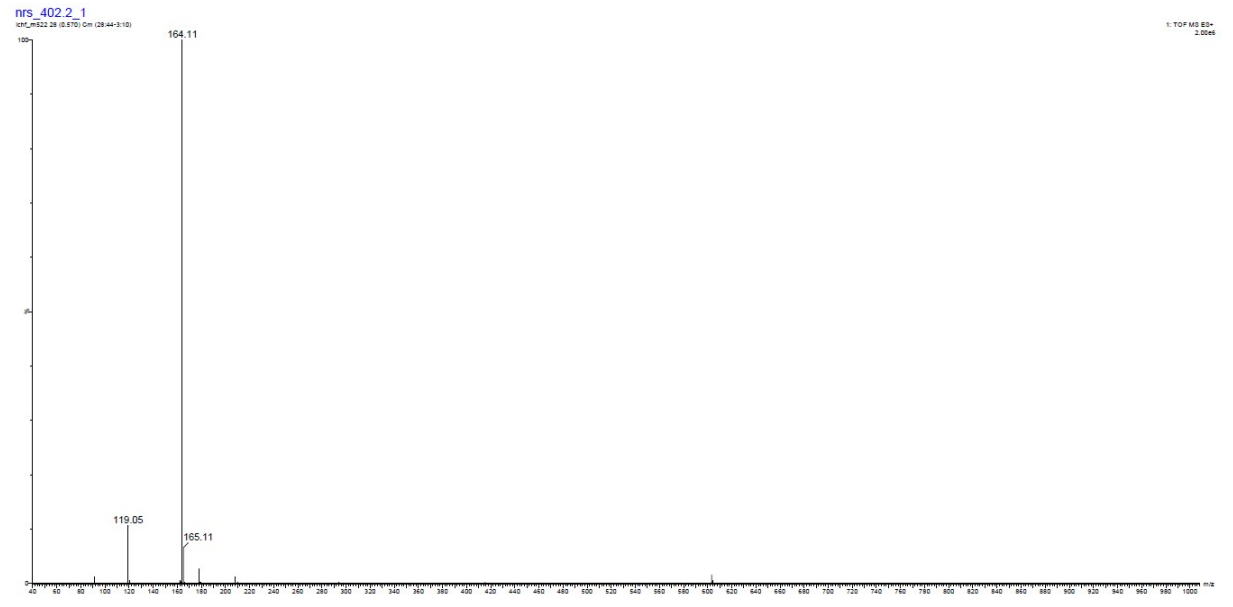

Figure S19. Mass spectrum of **6** under electrospray ionization in positive ion mode.

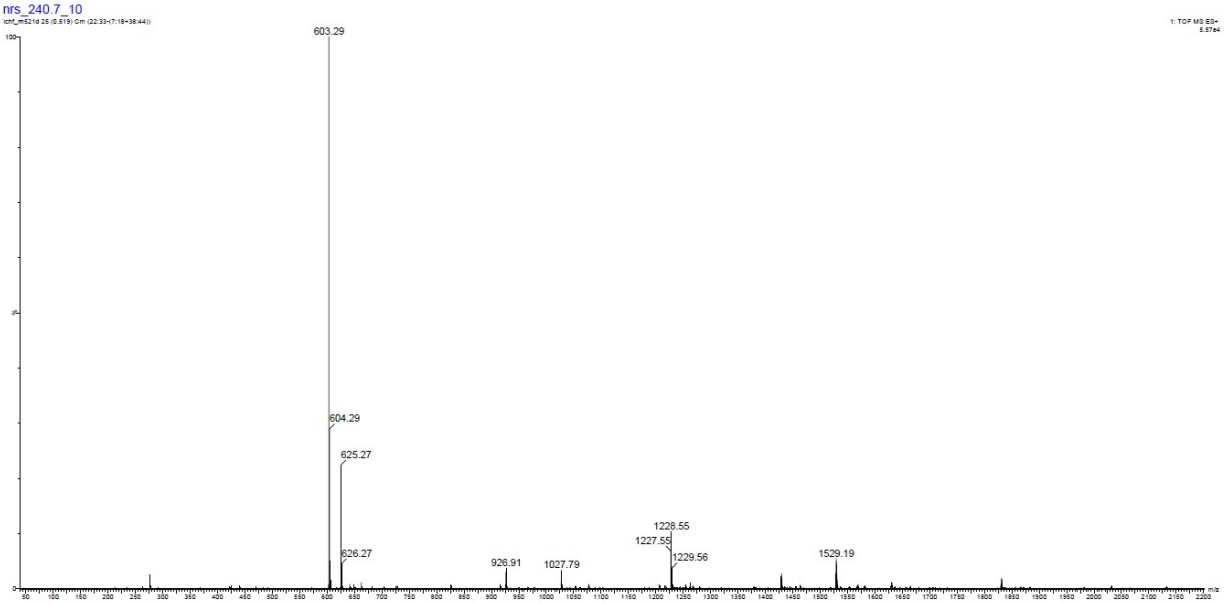

Figure S20. Mass spectrum of **SP** under electrospray ionization in positive ion mode.

Figure S21. Mass spectrum of **Ald** under electrospray ionization in positive ion mode.

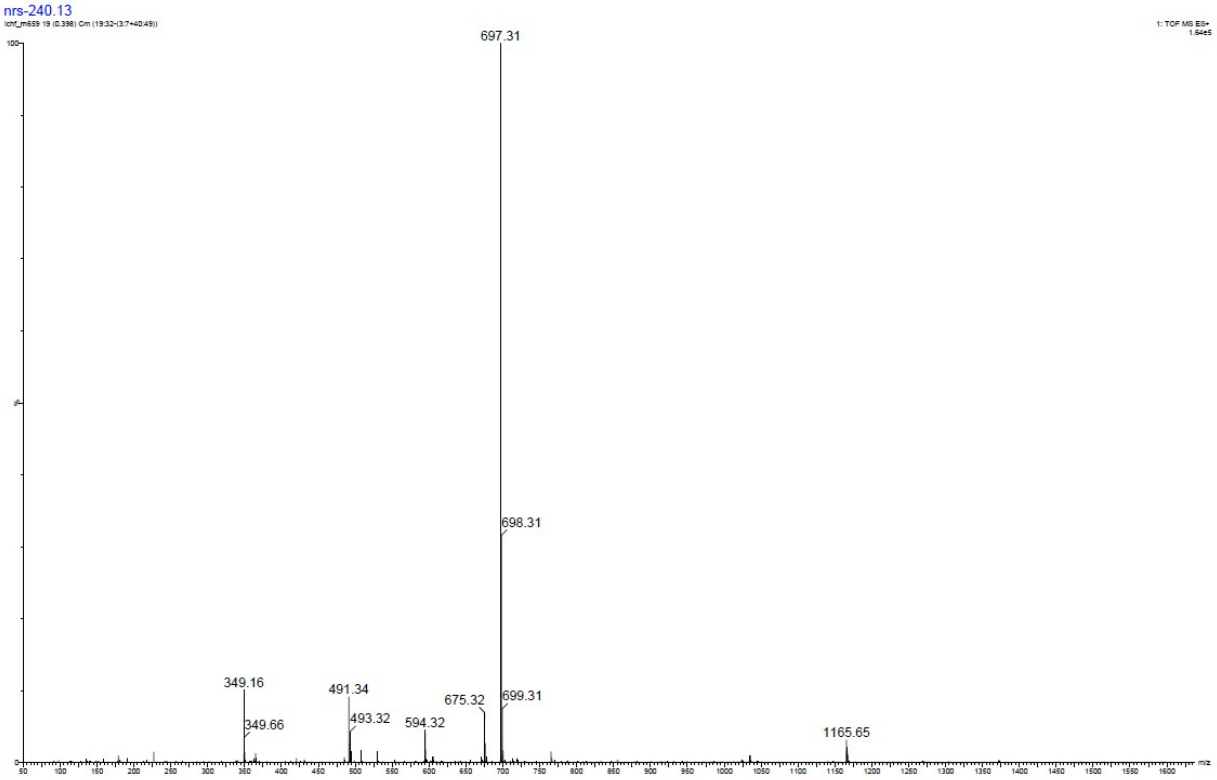

Figure S22. Mass spectrum of **SP-hydr** under electrospray ionization in positive ion mode.

3. Isomerization

Isomerization was studied by NMR spectroscopy. The proton NMR spectra made it possible to observe the isomerization of the less stable SP form into the more stable MCH form during thermal relaxation in the dark (Figure S23). Importantly, each photostationary state contained only one form, which promised high operation efficiency of the devised pseudorotaxane. Proton assignments were made based on COSY and ROESY spectra (Figures S11-12, S24-27).

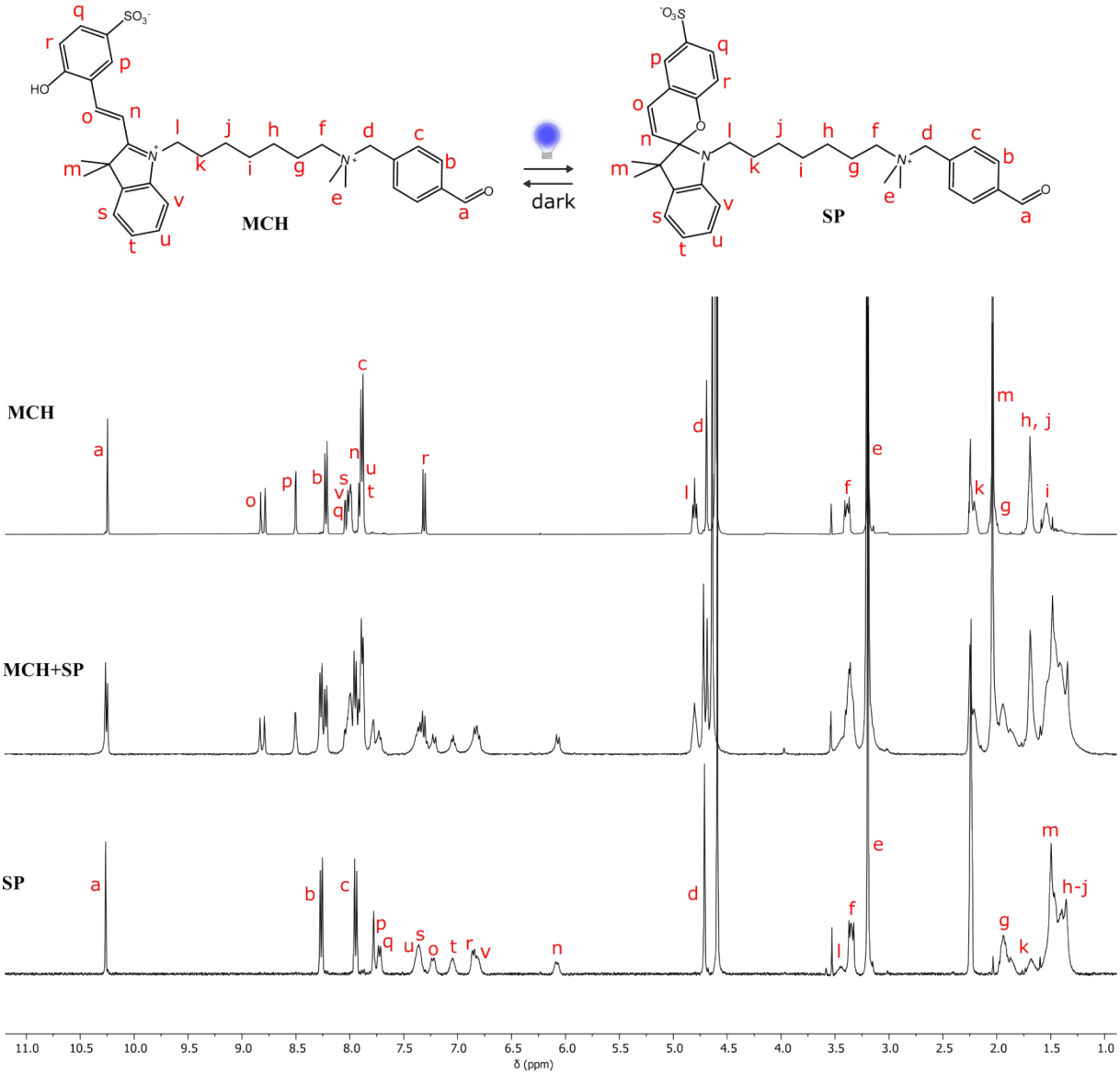

Figure S23. ^{1}H NMR spectra showing the isomerization of the SP form into the MCH form upon thermal relaxation in the dark (MeCN-d_3/D_2O, 298 K).

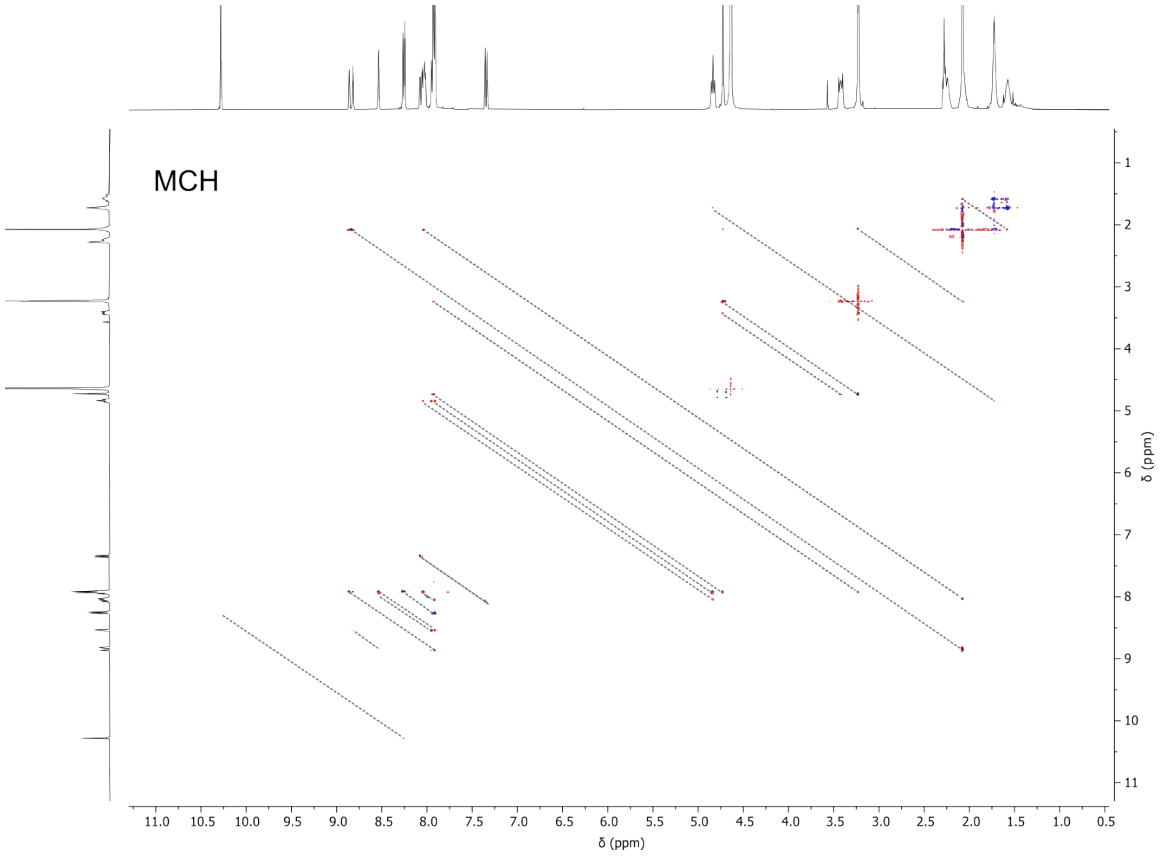

Figure S24. ROESY spectrum of the MCH form (MeCN-d_3/D_2O, 298 K).

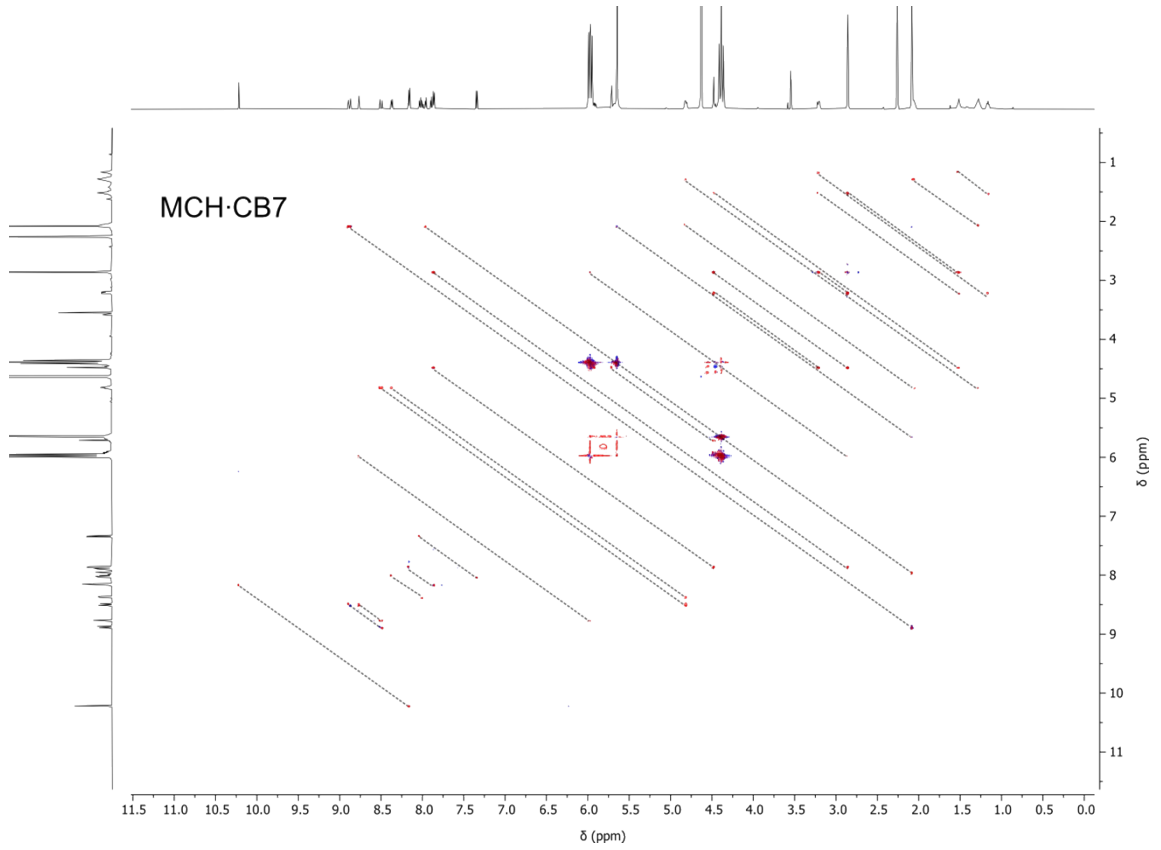

Figure S25. ROESY spectrum of the MCH form with 1 equiv. of CB7 (MeCN-d_3/D_2O, 298 K).

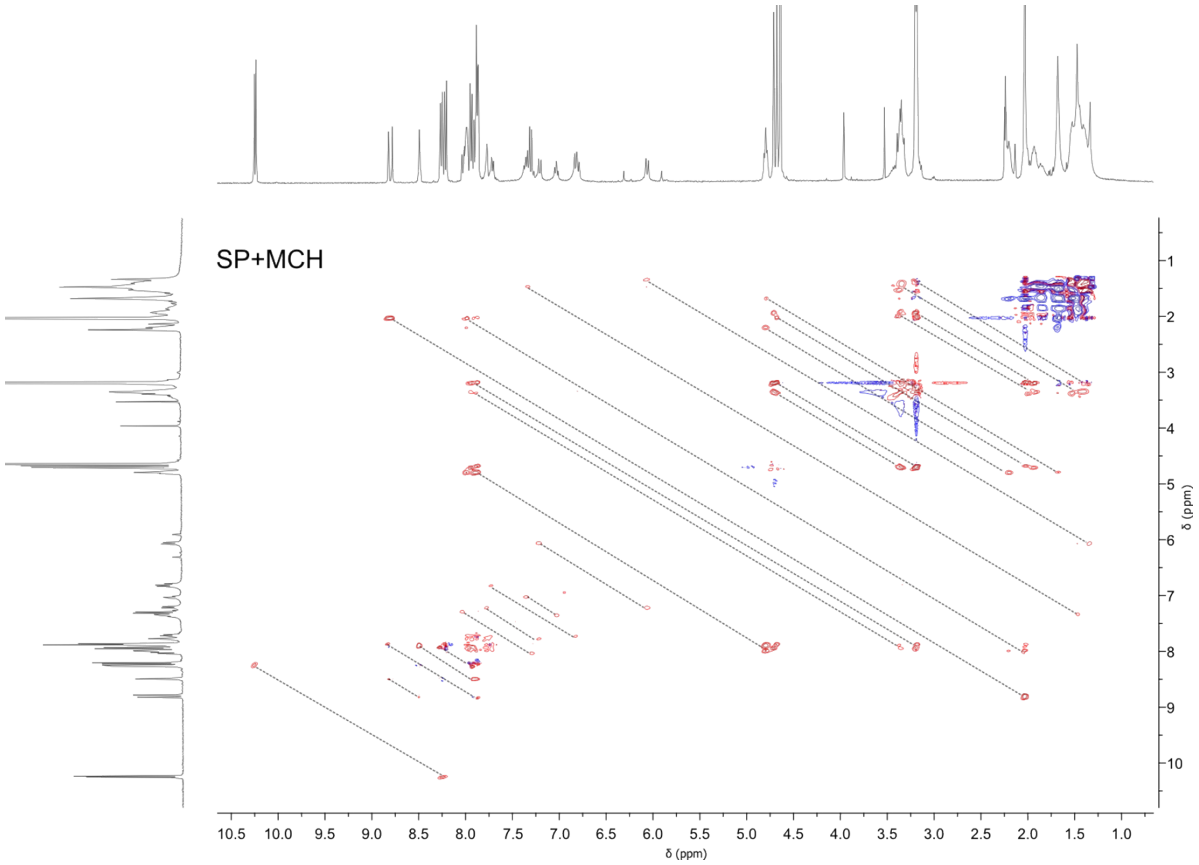

Figure S26. ROESY spectrum of a mixture of SP and MCH forms (MeCN-d_3/D_2O, 298 K).

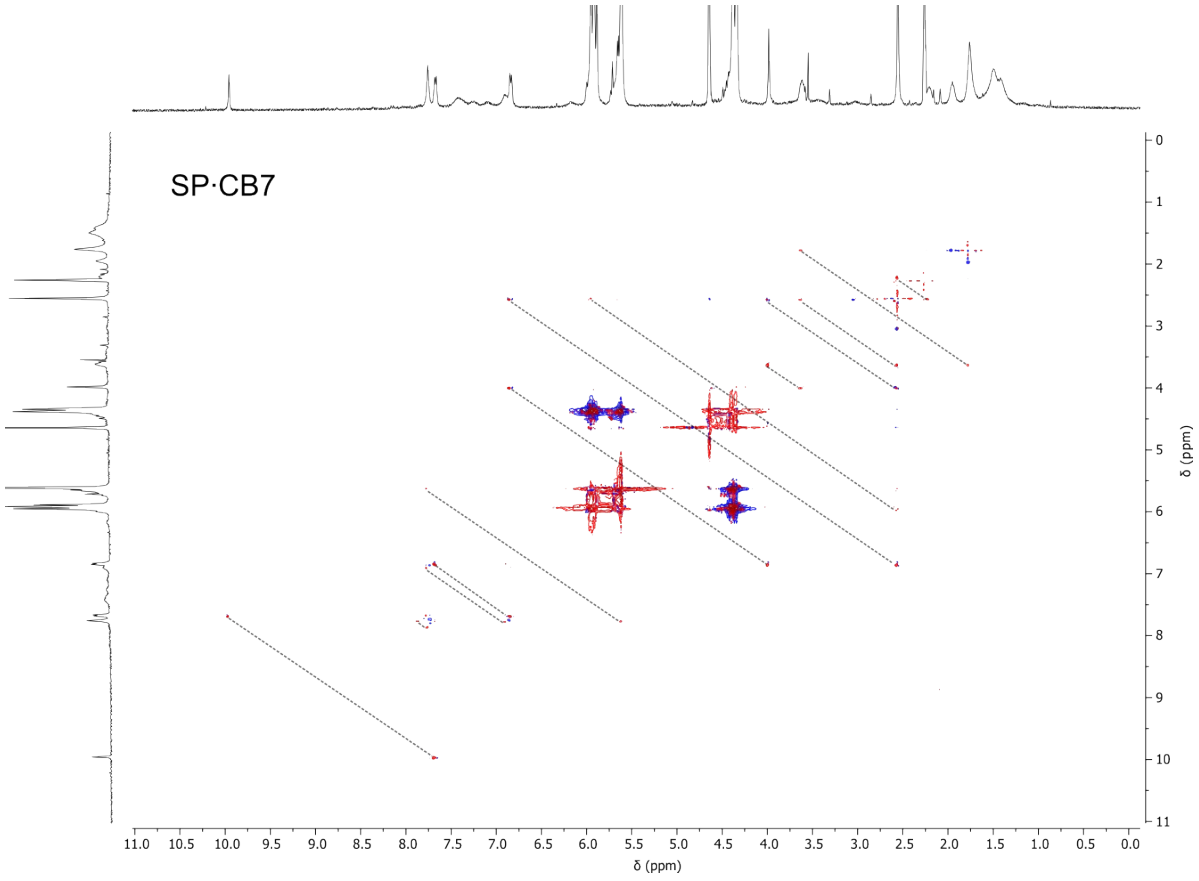

Figure S27. ROESY spectrum of the SP form with 1 equiv. of CB7 (MeCN-d_3/D_2O, 298 K).

Isomerization was also studied by UV-Vis spectroscopy. The formation of the MCH form was accompanied by the appearance of a new band at 420 nm (Figure S28). The use of light with a wavelength close to this value (430 nm) induced a rapid back isomerization (few seconds) to the SP form. To slow this process, we used a shorter wavelength (365 nm) of very low intensity (5% of maximum power), see Figure S29.

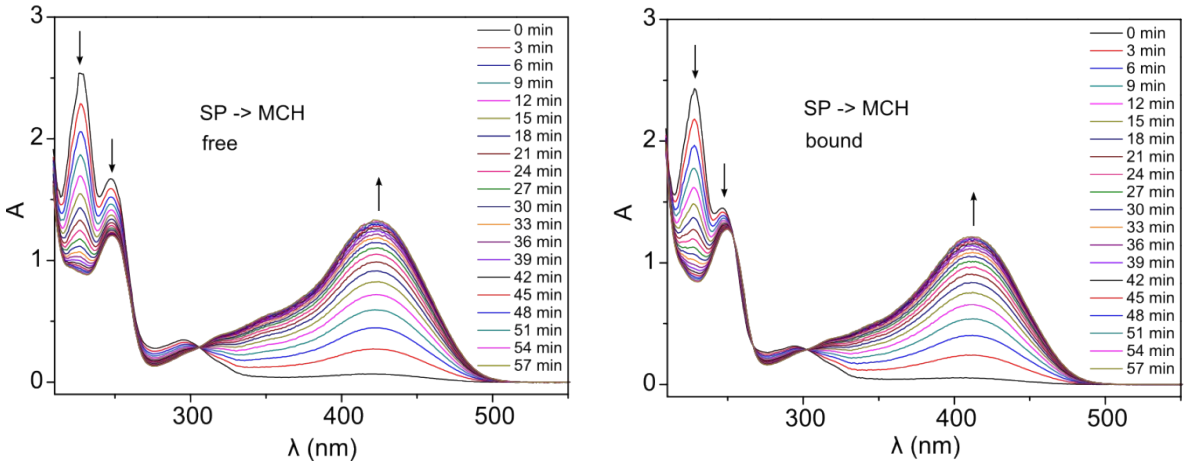

Figure S28. UV-Vis spectra showing the isomerization of the SP form into the MCH form upon thermal relaxation in the dark (MeCN/H_2O, 298 K).

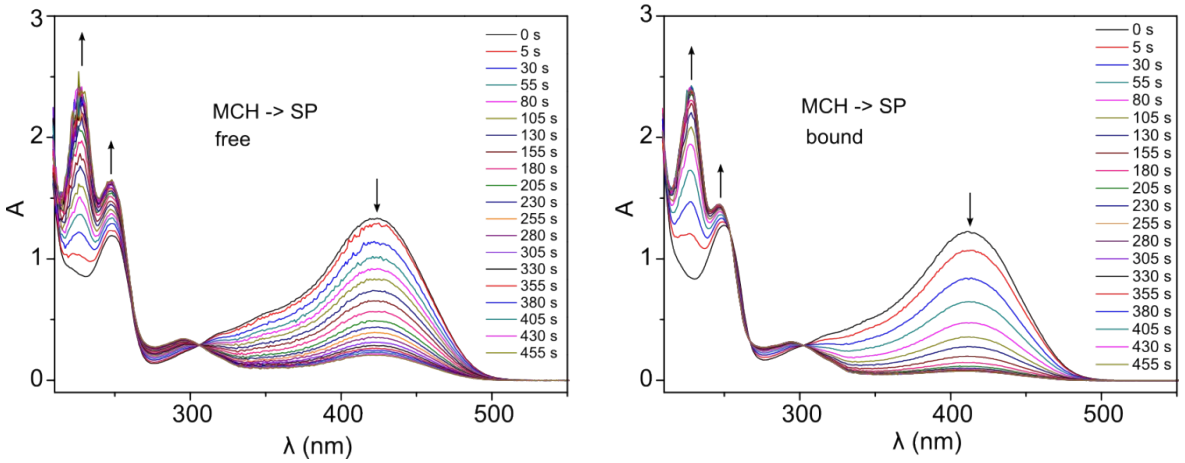

Figure S29. UV-Vis spectra showing the isomerization of the MCH form into the SP form upon UV light irradiation (MeCN/H_2O, 298 K).

UV-Vis spectroscopy has been also used to determine isomerization kinetics:

Solvent

Solvent was prepared by mixing 30 mL of H_2O with 30 mL of MeCN and adjusting to pH ≈ 3.0 with 2M HCl (15.0 µL).

Axle solution

1.38 mg of the axle was dissolved in 2.69 mL of solvent. A 2.4 mL portion was diluted with 36 mL of the solvent to give a 50 µM solution.

Macrocycle solution

9.54 mg of the macrocycle was dissolved in 848 µL of solvent to give a 7.5 mM solution.

Isomerization from SP to MCH form

The UV-Vis cuvette was filled with 1.5 mL of axle solution. Afterward, either 50 µL of solvent or 50 µL of macrocycle solution was added. The mixture was then irradiated for 1 min using a 365 nm LED at 50% maximum power to convert the axle into the SP form. Next, the solution was left in the dark and UV-Vis spectra were recorded at 1 min intervals (Figure S30). The experiment was halted when no changes in the intensity of the MCH form were observed.

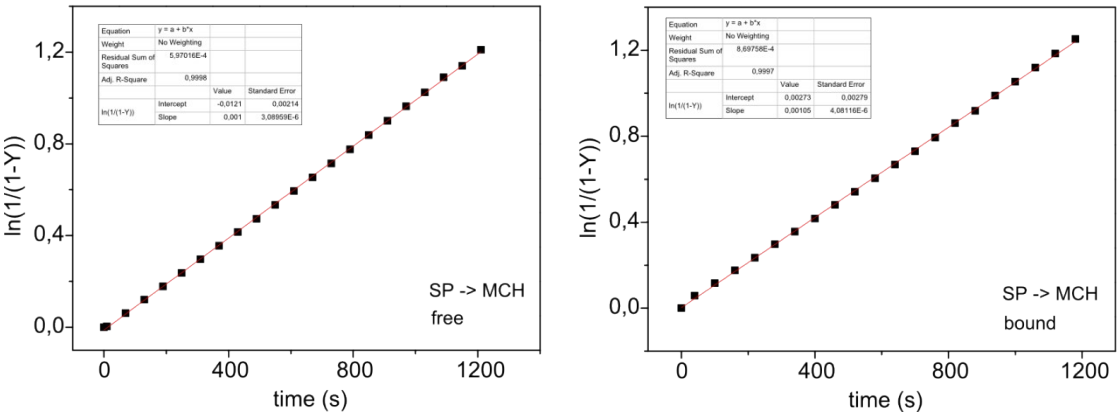

Figure S30. Kinetic traces showing the isomerization of the SP form into the MCH form upon thermal relaxation in the dark (MeCN/H_2O, 298 K).

Isomerization from MCH to SP form

The UV-Vis cuvette was filled with 1.5 mL of axle solution and left in the dark for 2 h to convert the SP form into the MCH form. Afterward, either 50 µL of solvent or 50 µL of macrocycle solution was added. The mixture was then irradiated using a 365 nm LED at 10% maximum power to prevent the back isomerization observed at 5% light intensity. The absorbance at 420 nm (maximum of MCH band) was recorded at 3 s intervals (Figure S31). The experiment was stopped when no changes in the intensity were observed.

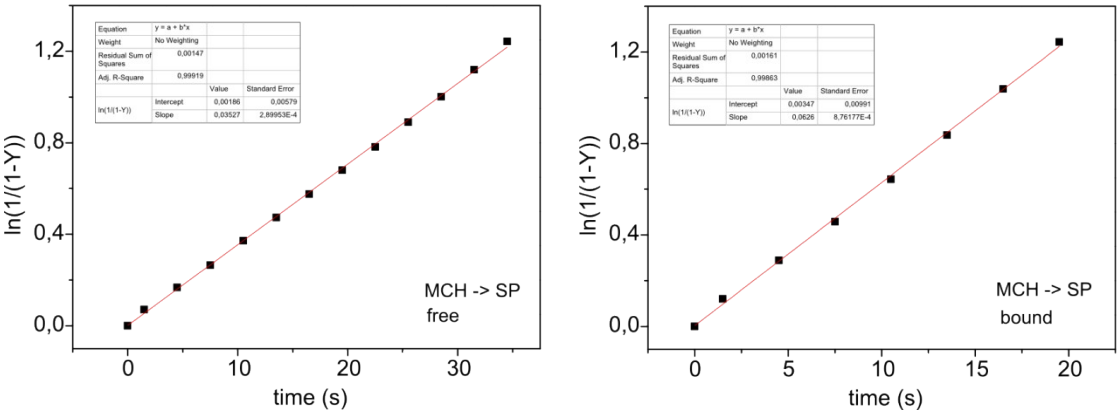

Figure S31. Kinetic traces showing the isomerization of the MCH form into the SP form upon blue light irradiation in the dark (MeCN/H_2O, 298 K).

The degree of isomerization was calculated as:

$$Y = \frac{A - A_0}{A_\infty - A_0}$$

where A is the absorbance at time *t*, A_0 is the absorbance at the beginning of the reaction, and A_∞ is the absorbance at 100% conversion.

Since the isomerization obeys first order kinetics, the isomerization rate was determined from:

$$ln\frac{1}{1-Y} = kt$$

The half-live of each species under these conditions can be obtained from:

$$t_{1/2} = \frac{ln2}{k}$$

Table S1. Kinetic parameters of isomerization.

sample	k (s^{-1})	$t_{1/2}$ (s)
SP_{free}	$1.00x10^{-3}$	693
SP_{bound}	$1.05x10^{-3}$	660
MCH_{free}	$3.53x10^{-2}$	20
MCH_{bound}	$6.26x10^{-2}$	11

4. Complexation

Initially, we thought to determine the binding constant directly from NMR titration. To this end, the axle (5 mg) was dissolved in D_2O (882 µL) and MeCN-d_3 (648 µL), and adjusted to pD ≈ 2.5 with DCl (0.1 M, 93 µL). A 400 µL of the prepared 4.5 mM solution was then transferred to the NMR tube and kept in the dark for 2 h so that the SP form could be converted to the MCH form. The solution was titrated with 9 mM solution of the macrocycle. In another experiment, the axle (5 mg) was dissolved in D_2O (955 µL) and MeCN-d_3 (648 µL), and adjusted to pD ≈ 2.5 with DCl (0.1 M, 20 µL. A 400 µL of the prepared 4.5 mM solution was then transferred to the NMR tube and titrated immediately with 9 mM solution of the macrocycle. During the titration, the sample was constantly irradiated with blue light to prevent the conversion of the SP form into the MCH form. In both experiments, no signal change was observed above 1 equiv. of the macrocycle, indicating a 1:1 binding stoichiometry (Figure S32-33). Unfortunately, slow proton exchange between bound and unbound species made it practically impossible to determine the binding constant. To address this issue, we began looking for a molecule that could bind to the macrocycle and then be displaced by the axle. The choice fell on the benzaldehyde derivative (Ald), which is a structural part of both MCH and SP forms. To prepare the stock solution for the titration, Ald (1.96 mg) was dissolved in D_2O (1.91 ml) and MeCN-d_3 (1.30 mL), and adjusted to pD ≈ 2.5 with DCl (0.1 M, 38 µL). A 500 µL of the prepared 4.2 mM solution was then transferred to the NMR tube and titrated with 16.2 mM solution of the macrocycle (prepared by dissolving 12.88 mg of CB7 in 511 µL of aldehyde solution). For NMR spectra, see Figure S34. The titration data points were fitted using BindFit software (http://supramolecular.org) to give the binding constant $K^{Ald} = (5.44 \pm 0.76) \cdot 10^4$ (Figure S35).

With this, we could find the binding strengths of SP and MCH by their displacement in a complex with benzaldehyde (Figures S36-37). Briefly, the axle (6.44 mg) and the macrocycle (15.33 mg) were dissolved in D_2O (697 µL) and MeCN-d_3 (538 µL), and adjusted to pD ≈ 2.5 with DCl (0.1 M, 110 µL). A 500 µL of the prepared 7.0 mM solution was transferred to the NMR tube. The sample was kept in the dark for 2 h to completely convert the axle to the MCH form. In parallel, 8.23 mg of Ald was dissolved in a mixture of D_2O (447 µL) and MeCN-d_3 (304 µL), and adjusted to pD ≈ 2.5 with DCl (0.1 M, 9 µL) to give a 7.0 mM solution. The MCH solution was titrated with aldehyde solution. In another experiment, the axle (5.98 mg) and the macrocycle (14.50 mg) were dissolved in a mixture of D_2O (737 µL)

and MeCN-d_3 (500 μL), and adjusted to pD ≈ 2.5 with DCl (0.1 M, 12 μL). A 500 μL of the prepared 7 mM solution was transferred to the NMR tube, and titrated with aldehyde solution prepared early. The titration was performed under constant blue light illumination (445 nm, 50% of maximum power).

The relative binding constants were calculated as follows:

$$SP + CB7 \rightleftharpoons SP \cdot CB7 \qquad K^{SP} = \frac{[SP \cdot CB7]}{[SP][CB7]}$$

$$MCH + CB7 \rightleftharpoons MCH \cdot CB7 \qquad K^{MCH} = \frac{[MCH \cdot CB7]}{[MCH][CB7]}$$

$$Ald + CB7 \rightleftharpoons Ald \cdot CB7 \qquad K^{Ald} = \frac{[SP \cdot CB7]}{[SP][CB7]}$$

$$K_{rel}^{SP} = \frac{K^{SP}}{K^{Ald}} = \frac{[SP \cdot CB7]}{[SP]} \cdot \frac{[Ald]}{[Ald \cdot CB7]}$$

$$K_{rel}^{MCH} = \frac{K^{MCH}}{K^{Ald}} = \frac{[MCH \cdot CB7]}{[MCH]} \cdot \frac{[Ald]}{[Ald \cdot CB7]}$$

[MCH·CB7]/[MCH] was determined by integrating the proton resonance, denoted as **o**:

$$\frac{[MCH \cdot CB7]}{[MCH]} = \frac{I_c}{I_0}$$

where I_0 is the intensity at $[CB7] = 0$, I_c is the intensity at $[CB7] \neq 0$.

[Ald·CB7]/[Ald] was determined from shifting of the proton resonance, denoted as **e**:

$$\frac{[Ald \cdot CB7]}{[Ald]} = \frac{\delta_0 - \delta_c}{\delta_\infty - \delta_0}$$

where δ_0 is the shift at $[CB7] = 0$, $\delta_\infty$is the shift at $[CB7] = \infty$, and δ_c is the shift at $[CB7] \neq 0$. The first two values were taken from the titration of Ald by CB7 (Figure S34). In practice, δ_∞ is equal to δ at $[CB7]/[Ald] > 1$, because after this point no further changes in the shift were observed.

Plotting [MCH·CB7]/[MCH] against [Ald·CB7]/[Ald] (Figure S38) gave a straight line with a slope of $K_{rel}^{MCH} = 1.62$. Hence, we get $K^{MCH} = 1.62 \cdot K^{Ald} = 8.81 \cdot 10^4$.

In the same way, we calculated the binding constant of the SP form with the difference that [SP·CB7]/[SP] was calculated by integrating the proton resonance, denoted as **e**. Plotting [SP·CB7]/[SP] against [Ald·CB7]/[Ald] (Figure S38) gave $K_{rel}^{SP} = 0.33$, and $K^{SP} = 0.33 \cdot K^{Ald} = 1.80 \cdot 10^4$, correspondingly.

The amount of pseudorotaxane in the solution was calculated as follows. In the dark, after mixing the axle and the macrocycle, a chemical equilibrium is established between the more stable MCH form and the macrocycle, which can be expressed:

$$K_d^{MCH} = \frac{[MCH][CB7]}{[MCH \cdot CB7]}$$

where $[MCH]$, $[CB7]$ and $[MCH \cdot CB7]$ are equilibrium concentrations of each species, and Kd is the dissociation constant.

Equilibrium concentrations can be also written as:

$$[MCH] = C_{MCH} - [MCH \cdot CB7]$$

$$[CB7] = C_{CB7} - [MCH \cdot CB7]$$

where C_{MCH} and C_{CB7} are the initial concentrations of MCH and CB7, respectively.

Inserting them into the chemical equilibrium equation

$$K_d^{MCH} = \frac{(C_{MCH} - [MCH \cdot CB7])(C_{CB7} - [MCH \cdot CB7])}{[MCH \cdot CB7]}$$

we obtain a quadratic equation with one unknown $[MCH \cdot CB7]$:

$$[MCH \cdot CB7]^2 - [MCH \cdot CB7]\left(C_{MCH} + C_{CB7} + K_d^{MCH}\right) + C_{MCH}C_{CB7} = 0$$

The solution of this equation gives:

$$[MCH \cdot CB7] = \frac{\left(C_{MCH} + C_{CB7} + K_d^{MCH}\right) - \sqrt{(C_{MCH} + C_{CB7} + K_d^{MCH})^2 - 4C_{MCH}C_{CB7}}}{2}$$

After substituting the association constant for the dissociation constant

$$K_d^{MCH} = \frac{1}{K^{MCH}}$$

the equation takes the following form:

$$[MCH \cdot CB7] = \frac{\left(C_{MCH} + C_{CB7} + \frac{1}{K^{MCH}}\right) - \sqrt{(C_{MCH} + C_{CB7} + \frac{1}{K^{MCH}})^2 - 4C_{MCH}C_{CB7}}}{2}$$

Having an equilibrium concentration, we can get a molar fraction of the assembled pseudorotaxane in solution:

$$X_{MCH \cdot CB7} = \frac{[MCH \cdot CB7]}{C_{MCH}}$$

In the same manner, we can obtain a molar fraction of the pseudorotaxane in the SP form (under irradiation).

For NMR experiments carried out at $C_{CB7} = 5.25\ mM$ and $C_{MCH} = C_{SP} = 5mM$, $X_{MCH \cdot CB7} = 0.972$ and $X_{SP \cdot CB7} = 0.921$, respectively. The molar fractions of pseudorotaxane in UV-Vis experiments ($C_{MCH} = C_{SP} = 50\mu M$) at different amounts of the macrocycle are summarized in Table S2.

Table S2. Molar fractions of the assembled pseudorotaxane in solution depending on the amount of CB7 used.

CB7 equiv.	$X_{MCH \cdot CB7}$	$X_{SP \cdot CB7}$
10	0.976	0.892
7.5	0.967	0.858
5	**0.947**	**0.792**
2.5	0.878	0.629
1.5	0.766	0.480
1	0.625	0.365
0.75	0.513	0.293
0.5	0.369	0.209
0.25	0.195	0.112
0	0.000	0.000

The relative time that the macrocycle spends on the aromatic station in the OFF state, i.e., its molar fraction, can be calculated as:

$$x_{Ar}^{OFF} = \frac{\delta_{Al}^{OFF} - \delta_{mix}^{OFF}}{\delta_{Al}^{OFF} - \delta_{Ar}^{OFF}}$$

where δ_{Al}^{OFF} is the hypothetical shift of H_a, when the macrocycle is entirely located on the aliphatic station; δ_{Ar}^{OFF} is the hypothetical shift of H_a, when the macrocycle is entirely located on the aromatic station; δ_{mix}^{OFF} is the average (observed) shift of H_a, i.e., when the macrocycle is located on both stations.

In the same way we can express the molar fraction of the macrocycle on the aromatic station in the ON state:

$$x_{Ar}^{ON} = \frac{\delta_{Al}^{ON} - \delta_{mix}^{ON}}{\delta_{Al}^{ON} - \delta_{Ar}^{ON}}$$

where δ_{Al}^{ON} is the hypothetical shift of H_a, when the macrocycle is entirely located on the aliphatic station; δ_{Ar}^{ON} is the hypothetical shift of H_a, when the macrocycle is entirely located

on the aromatic station; δ_{mix}^{ON} is the average (observed) shift of H_a, i.e., when the macrocycle is located on both stations.

Since the macrocycle on the aliphatic station should not affect the chemical shift of distant H_a, and the macrocycle on the aromatic station should affect the chemical shift of H_a to the same degree, we get $\delta_{Ar}^{ON} \approx \delta_{Ar}^{OFF}$ and $\delta_{Al}^{ON} \approx \delta_{Al}^{OFF} \approx \delta$, where δ is the shift of H_a without the macrocycle. This approximation leads us to:

$$\frac{x_{Ar}^{ON}}{x_{Ar}^{OFF}} = \frac{\delta - \delta_{mix}^{ON}}{\delta - \delta_{Ar}^{ON}} \cdot \frac{\delta - \delta_{Ar}^{ON}}{\delta - \delta_{mix}^{OFF}} = \frac{\delta - \delta_{mix}^{ON}}{\delta - \delta_{mix}^{OFF}}$$

Substituting the experimental values ($\delta = 10.30$, $\delta_{mix}^{ON} = 9.98$, and $\delta_{mix}^{OFF} = 10.24$), we calculated the relative ratio as 5.26.

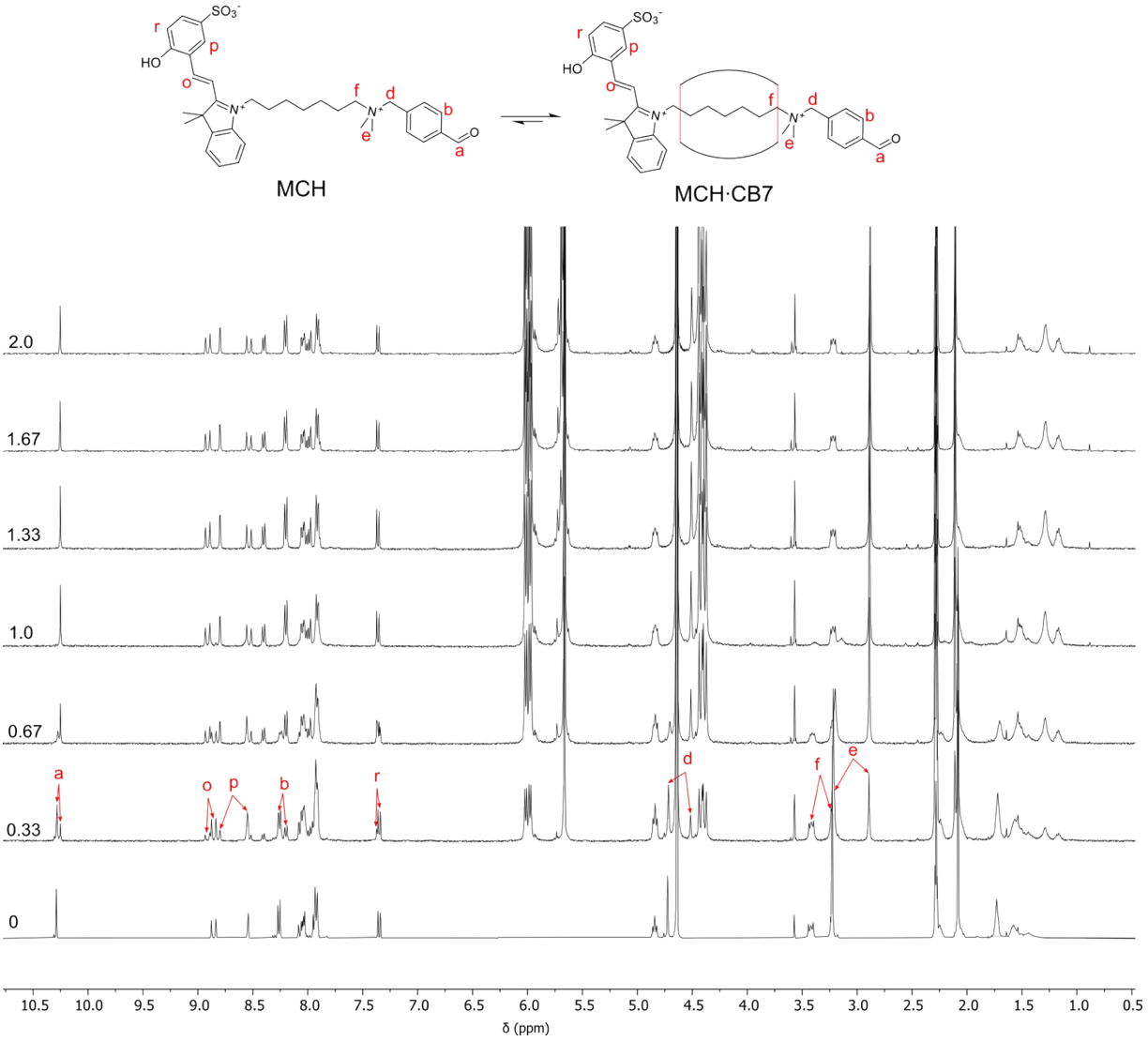

Figure S32. ^{1}H NMR spectra of MCH with increasing amounts of CB7 (MeCN-d_3/D_2O, 298 K).

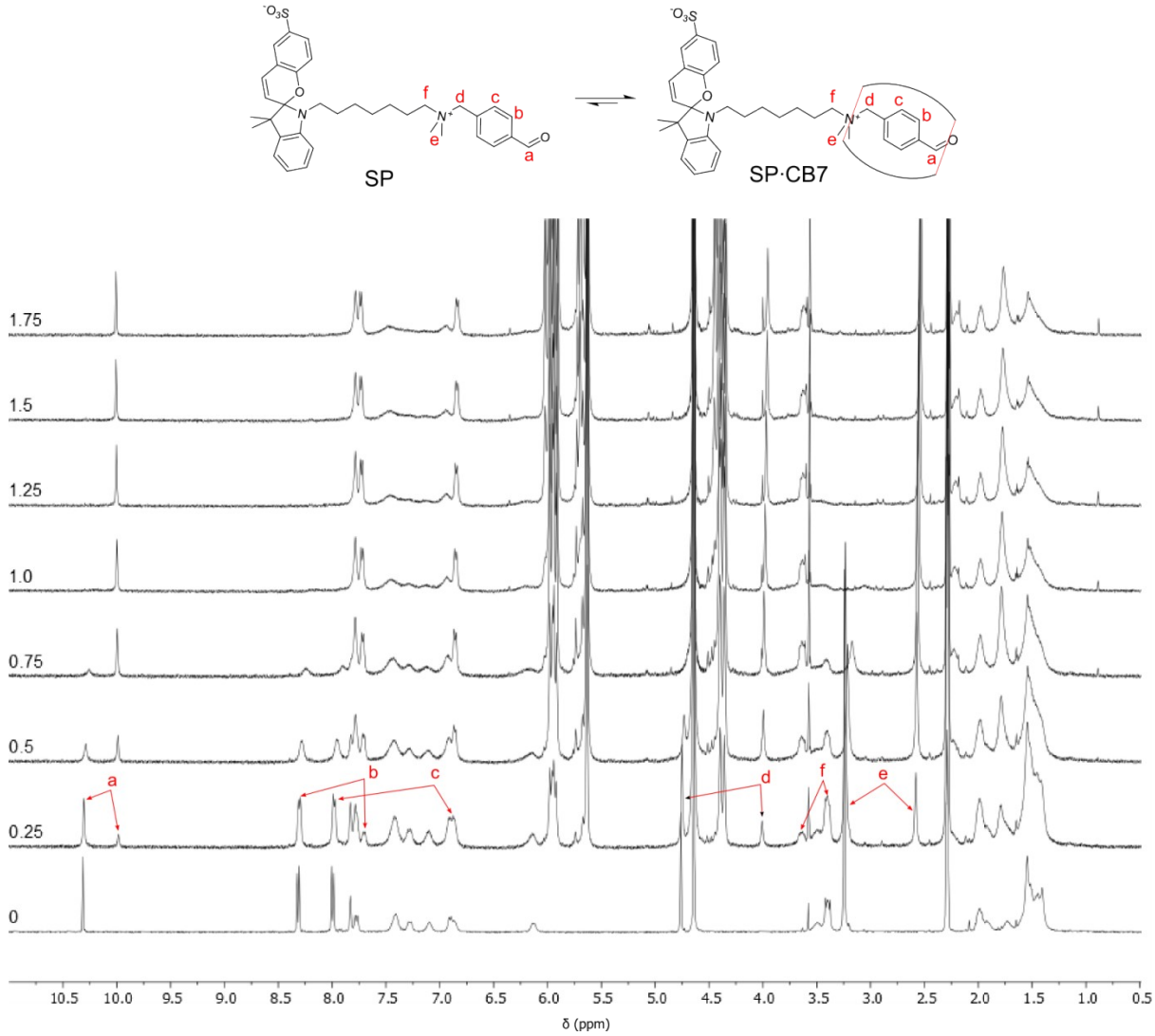

Figure S33. ^{1}H NMR spectra of SP with increasing amounts of CB7 (MeCN-d_3/D_2O, 298 K).

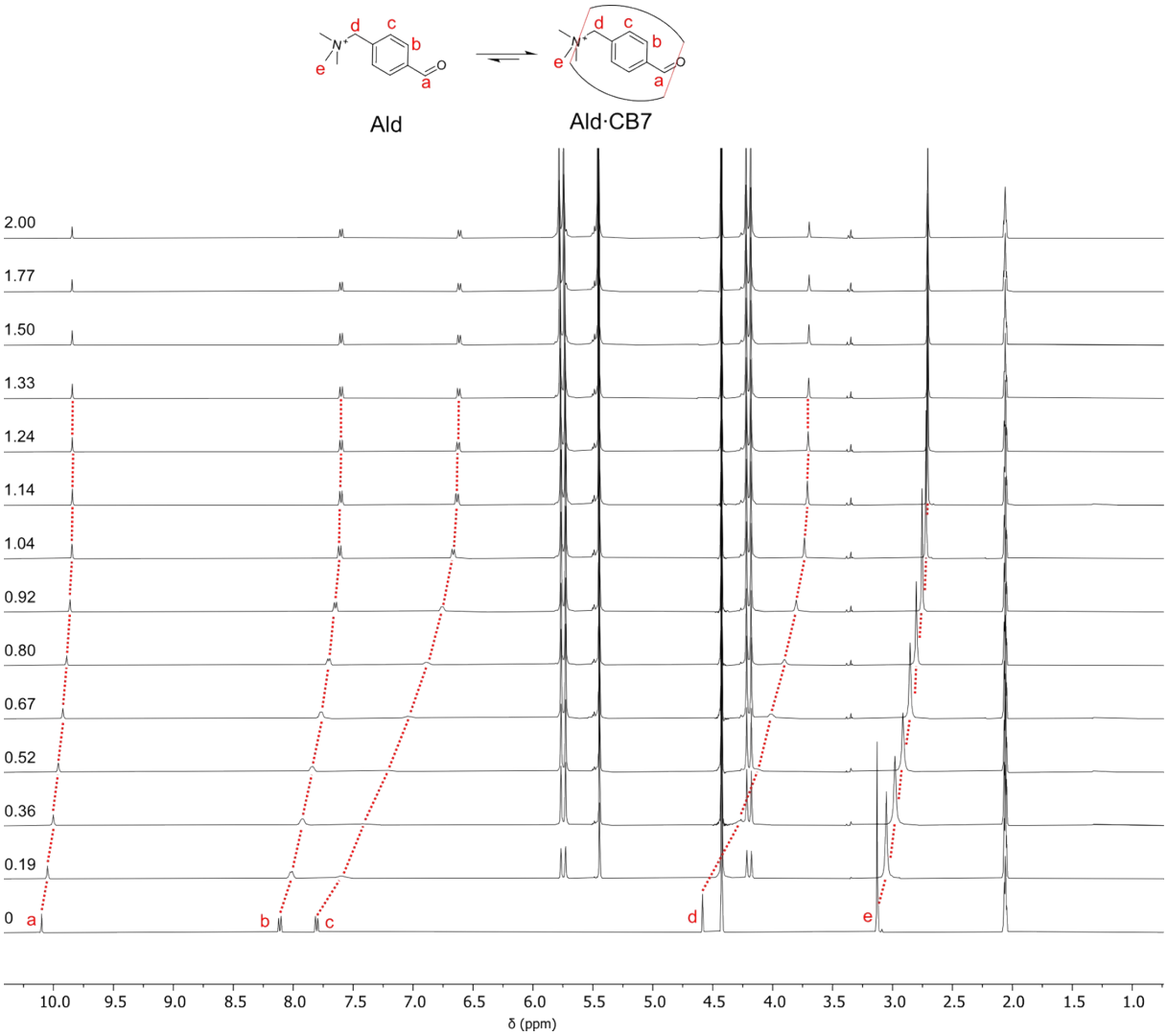

Figure S34. ^{1}H NMR spectra of Ald with increasing amounts of CB7 (MeCN-d_3/D_2O, 298 K).

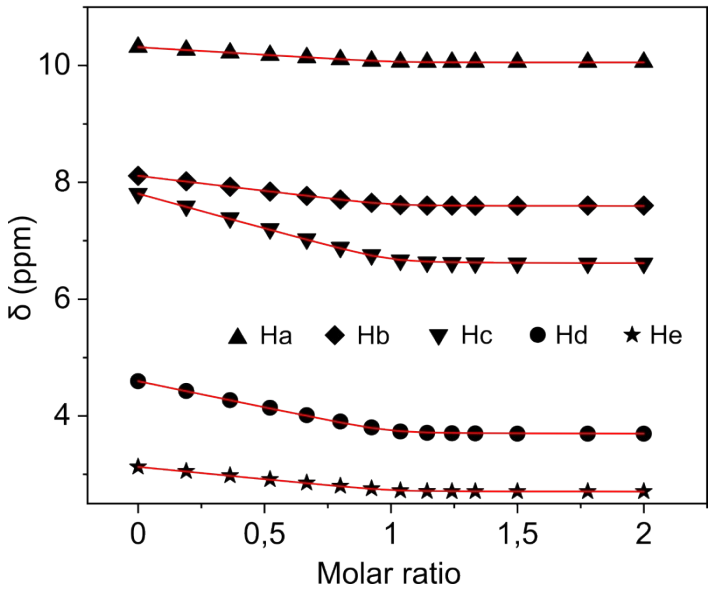

Figure S35. Non-linear fits of the data obtained from the titration of Ald by CB7.

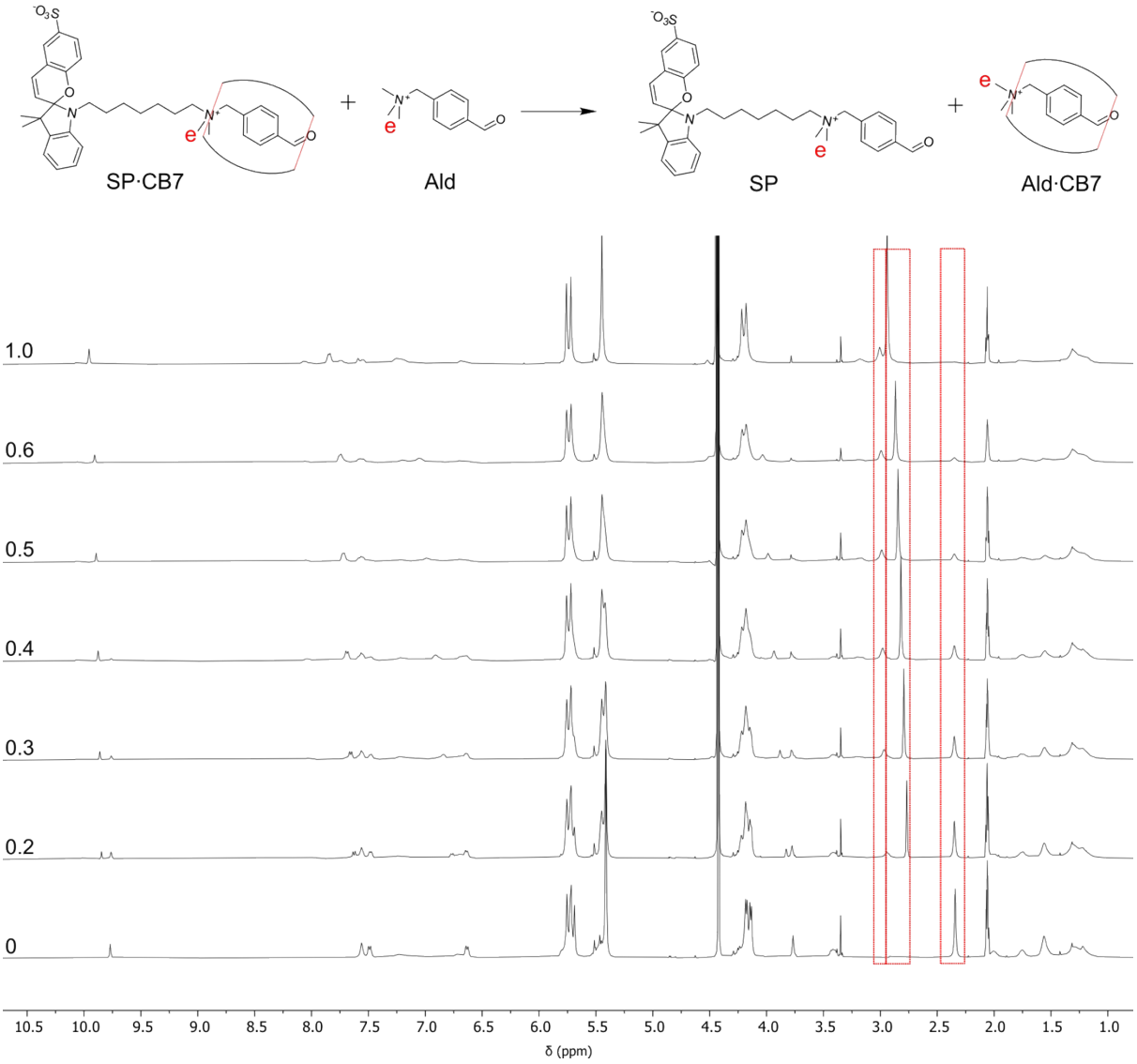

Figure S36. ^{1}H NMR displacement experiments of SP for Ald (MeCN-d_3/D_2O, 298 K).

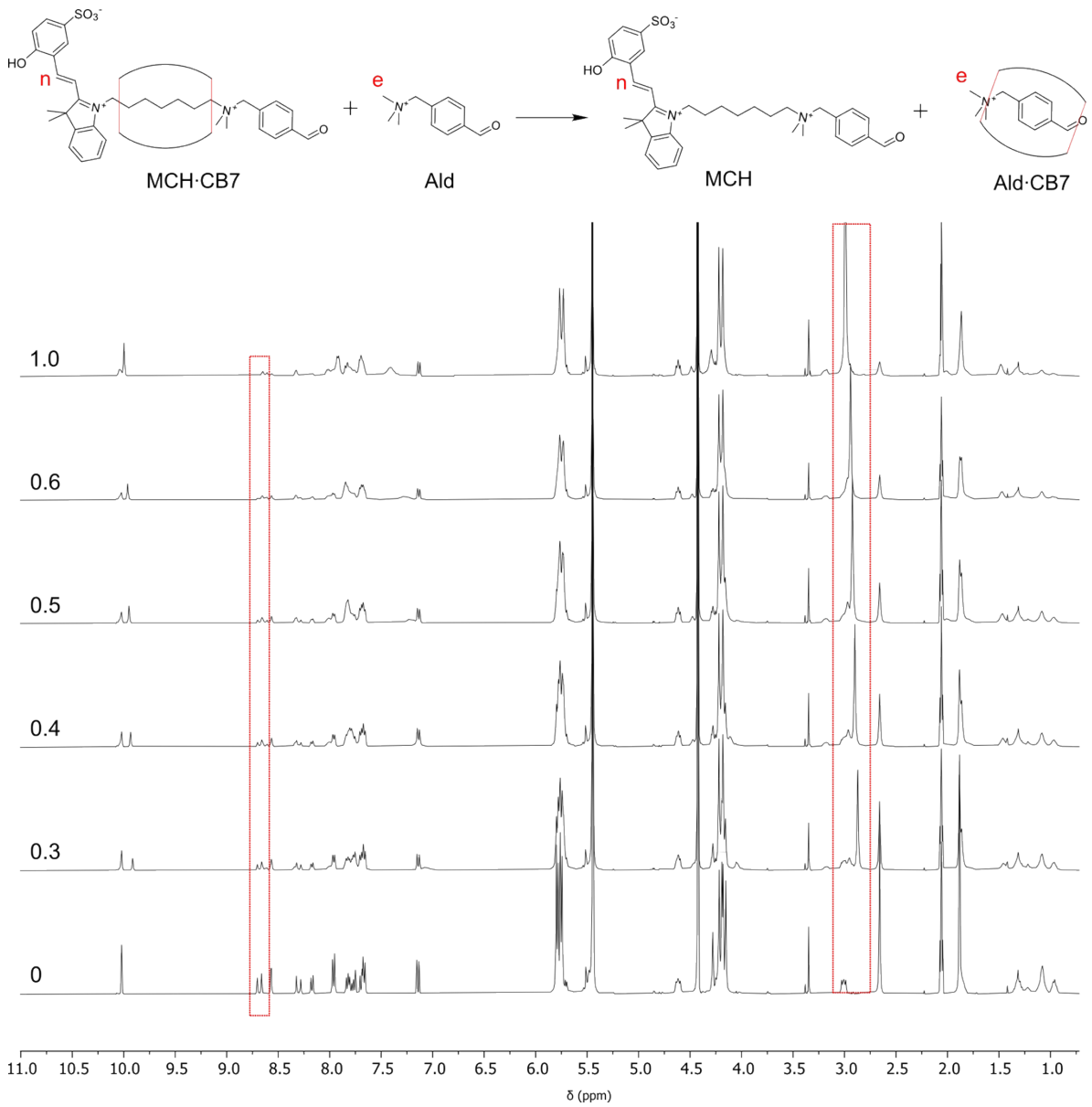

Figure S37. ^{1}H NMR displacement experiments of MCH for Ald (MeCN-d_3/D_2O, 298 K).

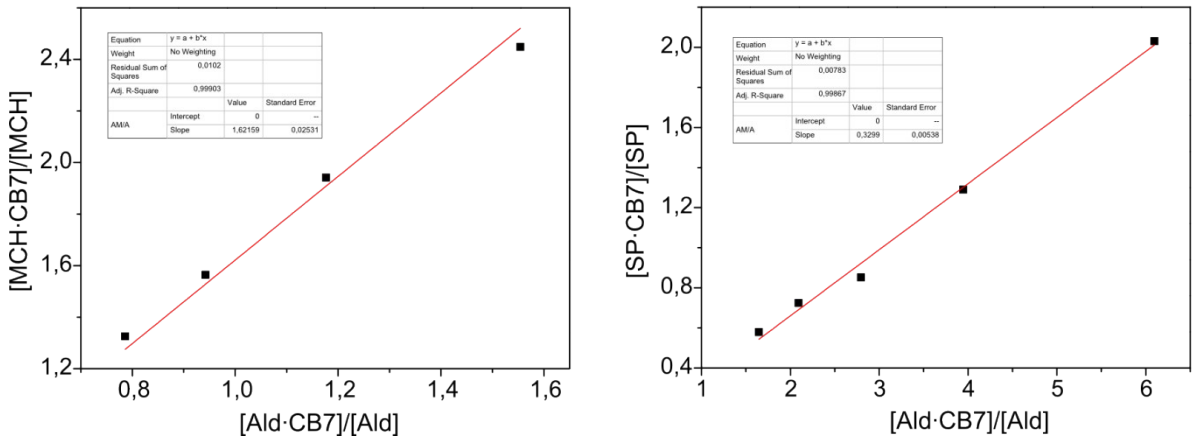

Figure S38. Determination of relative binding constants.

5. Hydrazonation

To determine at which pH the hydrazide would have the greatest buffering capacity, we determined its acidity by titration with aq. hydrochloric acid (see below). It was found that the $pK_a \approx 3.2$, so all experiments were performed at a pH close to this value.

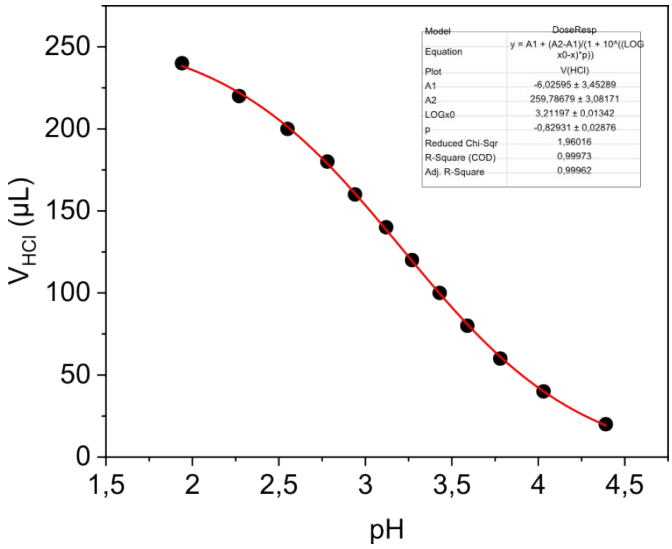

Figure S39. Titration of methyl hydrazinocarboxylate with hydrochloric acid.

Solvent

Solvent was prepared by mixing 30 mL of H_2O with 30 mL of MeCN and adjusting to pH ≈ 3.2 with 2M HCl (9.5 µL).

Hydrazide solution

11.25 mg of methyl hydrazinocarboxylate was dissolved in 4.16 mL of solvent, and adjusted to pH ≈ 3.0 with 30 µL of 2M HCl to give a 30 mM solution.

Axle solution

1.63 mg of SP was first dissolved in 3.18 mL of solvent. A 2.4 mL portion was diluted next with 36 mL of solvent to give a 50 µM solution.

Macrocycle solution

13.76 mg of CB7 was dissolved in 1.33 mL of solvent to give a 7.5 mM solution.

Hydrazonation of the pseudorotaxane (MCH form)

A UV-Vis cuvette was filled with 1.5 mL of axle solution and, if necessary, with the appropriate amount of macrocycle solution and left in the dark for 2 h to convert the SP form

into the MCH form. Next, 50 µL of hydrazide solution was added, and the absorbance at 282 nm was recorded every 3 s.

Hydrazonation of the pseudorotaxane(SP form)

A UV-Vis cuvette was filled with 1.5 mL of axle solution and, if necessary, with the appropriate amount of macrocycle solution. The solution was irradiated for 1 min using a 430 nm LED at 20% maximum power to convert the entire axle to the SP form. Immediately after that, the UV-Vis spectrum was recorded to determine A_0. Then, 50 µL of hydrazide solution was added, and absorbance at 282 nm (maximum of hydrazone band) was recorded at ~ 4 s intervals. Within these intervals, the sample was irradiated with a 430 LED at 20% maximum power.

The reaction rate was calculated in respect to the product (hydrazone), on which the reaction shows a pseudo-first-order dependence due to a large excess of hydrazide. The product yield was calculated as follows:

$$Y = \frac{A - A_0}{A_\infty - A_0}$$

where A is the absorbance at a time t, A_0 is the absorbance at the beginning of the reaction, and A_∞ is the absorbance at 100% conversion.

The rate constant was calculated as the slope of the function:

$$ln\frac{1}{1-Y} = kt$$

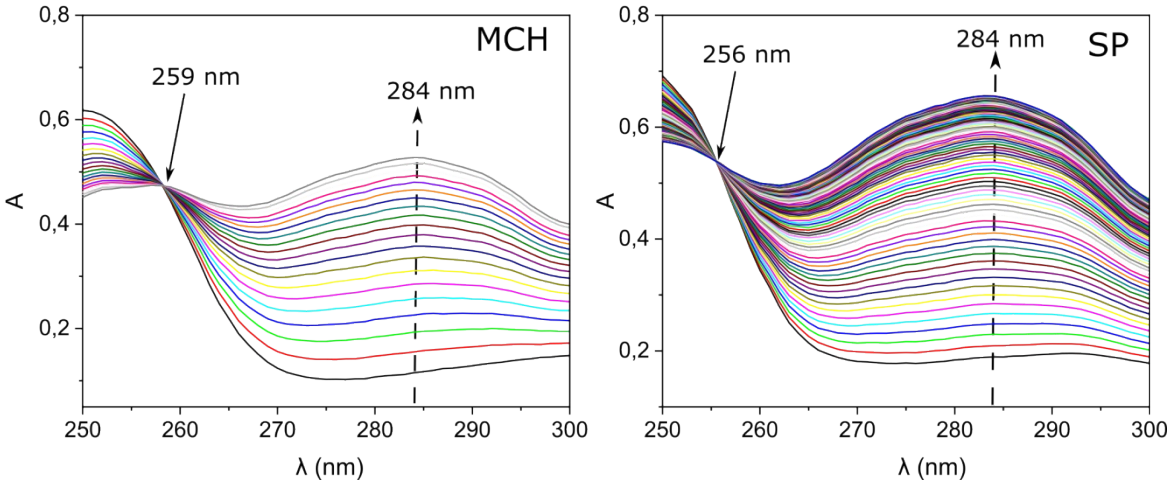

Fig S40. Partial spectra of hydrazonation of the pseudorotaxane with 5 eq. CB7 at pH 3.0. The dashed arrows show the increase of the hydrazone band. The presence of isosbestic points indicates no side reactions.

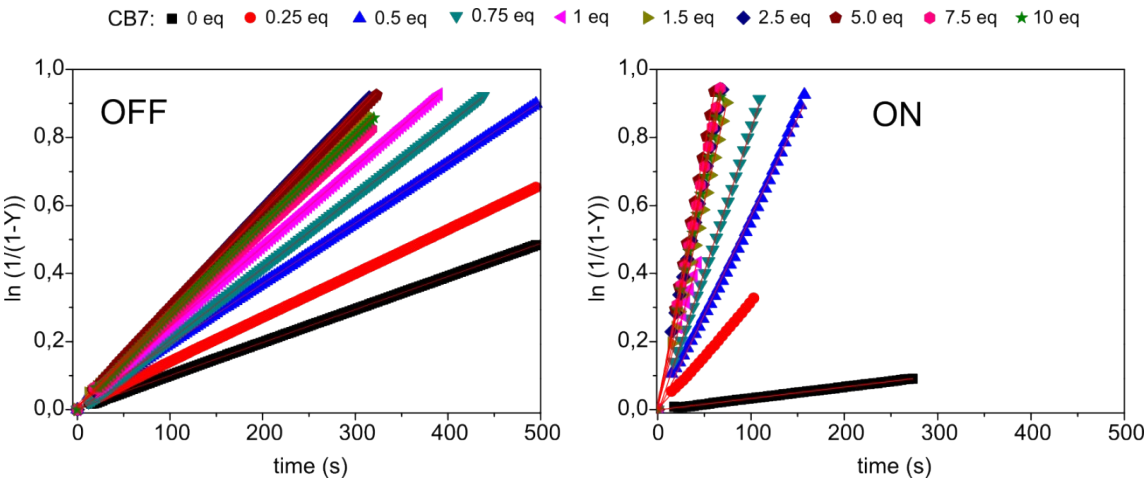

Figure S41. Kinetic traces for hydrazonation of the pseudorotaxane in MCH and SP forms at different amounts of CB7.

Table S3. Rate constants and acceleration factors for MCH and SP hydrazonation at different amounts of CB7.

CB7 eq	k(MCH), s^{-1}	k(SP), s^{-1}	k(SP)/k(MCH)
10	0.00267	0.01362	5.10
7.5	0.00259	0.01396	5.39
5	**0.00283**	**0.01524**	**5.39**
2.5	0.00291	0.01327	4.56
1.5	0.00275	0.01225	4.45
1	0.00236	0.01002	4.25
0.75	0.00213	0.00816	3.83
0.5	0.00179	0.00541	3.02
0.25	0.0013	0.00314	2.42
0	0.00097	0.000347	0.36

Pseudorotaxane recovery

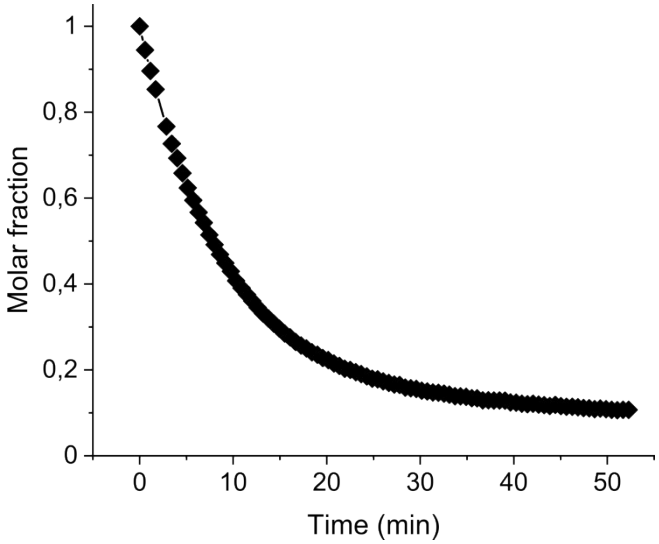

Figure S42. Kinetic traces for the hydrolysis of SP-hydrazone in the presence of CB7 at pH=2.

Controlling the outcome of concurrent reactions

Axle (5.19 mg, 1 equiv.), 4-nitrobenzaldehyde (1.15 mg, 1 equiv.), CB7 (12.78 mg, 1.1 equiv.) and an internal standard (1,3,5-benzenetricarboxylic acid, 0.7 mg, 0.44 equiv.) were weighed in a vial (4 ml) and dissolved in an ACN-D_2O mixture (843+1264 μL). 500 μL of the solution was then transferred into the NMR-tube and kept under irradiation (pH of the solution was measured as ≈ 3.0). In parallel, another NMR-tube with 500 μL of the solution was prepared, adjusted to pH ≈ 3.0 with 12 μL of 0.1 M solution of DCl in ACN-D_2O (600+400 μL) and kept in the dark.

The solution of hydrazides was prepared by dissolving of 1.13 mg (0.75 equiv.) of methyl hydrazinocarboxylate and 1.33 mg (0.75 equiv.) of semicarbazide hydrochloride in ACN-D_2O (560+373 μL). The pH of the solution was adjusted to ≈ 3.0 by the addition of 50 μL of 0.1 M solution of DCl in ACN-D_2O (600+400 μL).

The experiment was commenced by the addition of 100 μL of the hydrazide mixture to each NMR tube. The reaction was complete (equilibrium was reached) after 15 min.

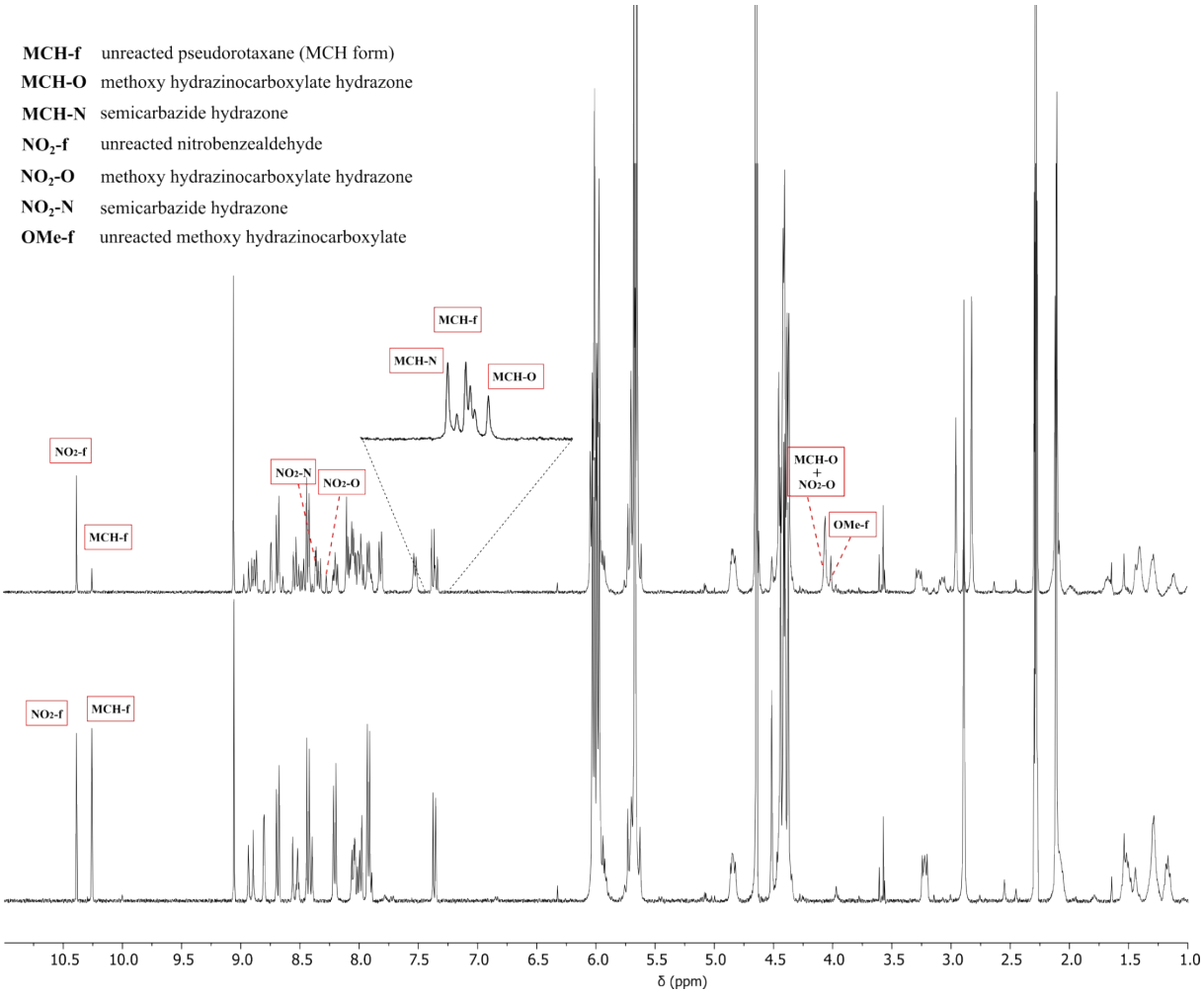

Figure S43. ^{1}H NMR spectra of the reaction mixture in the dark at the beginning of the reaction and after the equilibrium was established. The amount of unreacted pseudorotaxane and 4-nitrobenzaldehyde was found by integrating carbonyl proton resonances. The amount of 4-nitrobenzaldehyde hydrazones was calculated by integrating proton signals of –CH=N-R group. The amount of hydrazonated pseudorotaxane products was determined by integrating proton resonances of indole moiety.

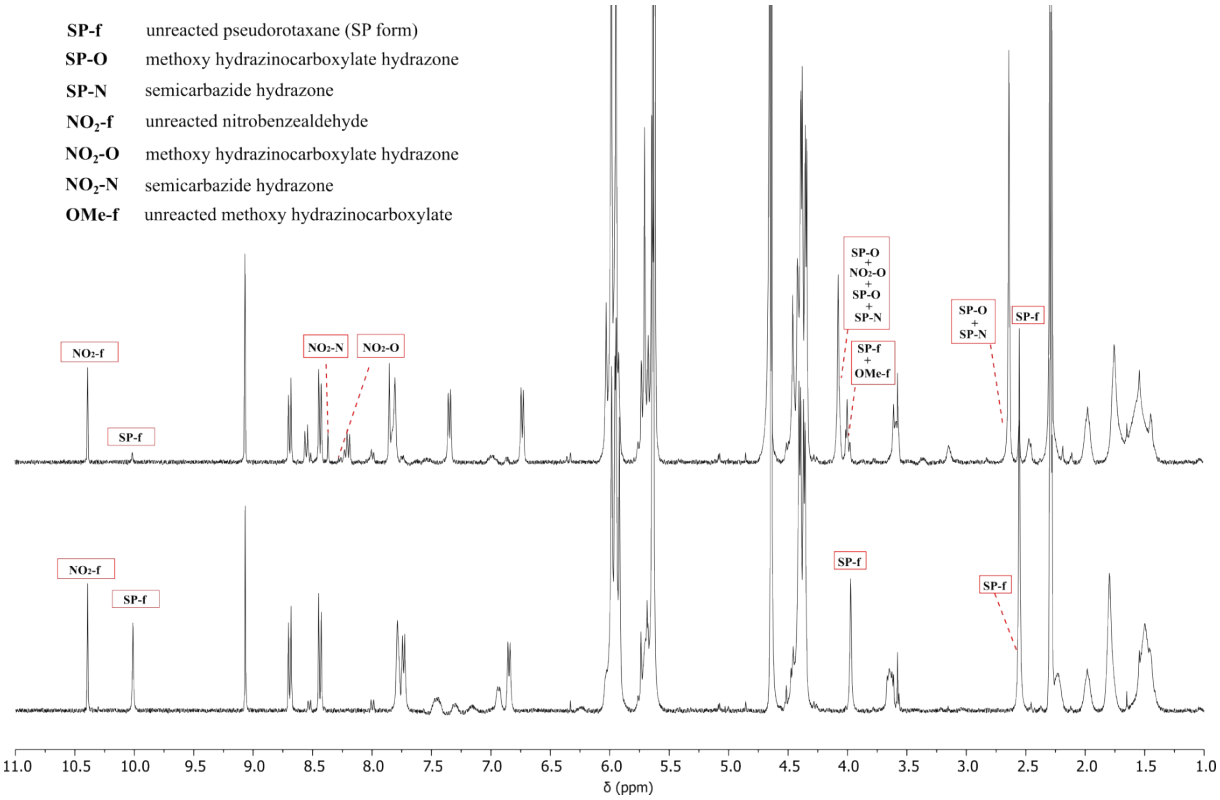

Figure S44. ^{1}H NMR spectra of the reaction mixture under irradiation at the beginning of the reaction and after the equilibrium was established. The amount of unreacted pseudorotaxane and 4-nitrobenzaldehyde was found by integrating carbonyl proton resonances. The amount of 4-nitrobenzaldehyde hydrazones was calculated by integrating proton signals of –CH=N-R group. The amount of SP-O was estimated based on the integrals of the proton signals of unreacted methoxy hydrazinocarboxylate and the formed NO_2-O. The amount of SP-N was determined by subtracting the estimated integral for SP-O from the total integral of SP reacted.

Table S4. Distribution of substrates and products in the reaction mixture under light and dark conditions.

	SP/MCH-O	SP/MCH-N	NO_2-O	NO_2-N	SP/MCH-f	NO_2-f
light	20	71	24	2	9	58
dark	30	51	21	8	19	56

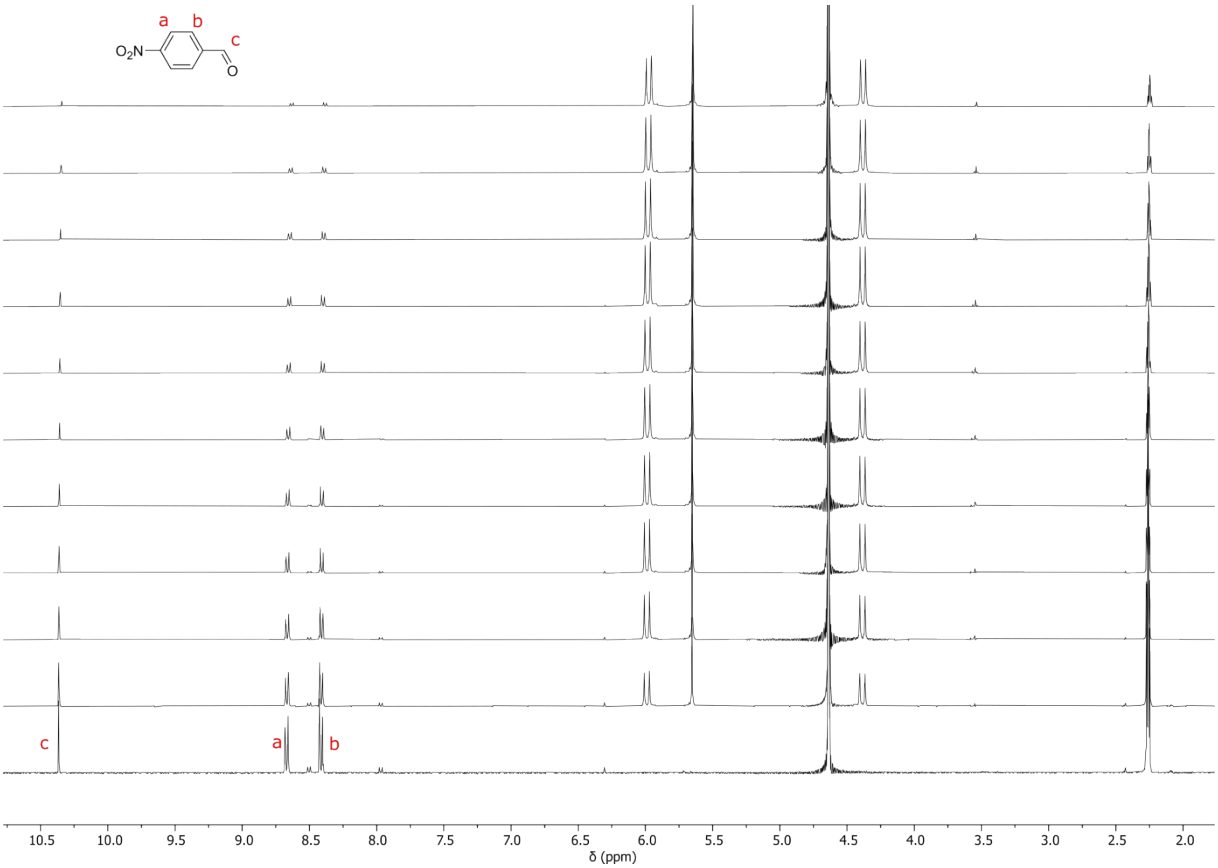

Figure S45. Titration of 4-nitrobenzaldehyde with increasing amounts of CB7 (0.00 0.14, 0.27, 0.39, 0.50, 0.69, 0.86, 1.00, 1.24, 1.50, 1.75 equiv.) in MeCN-d_3/D_2O at 298 K.

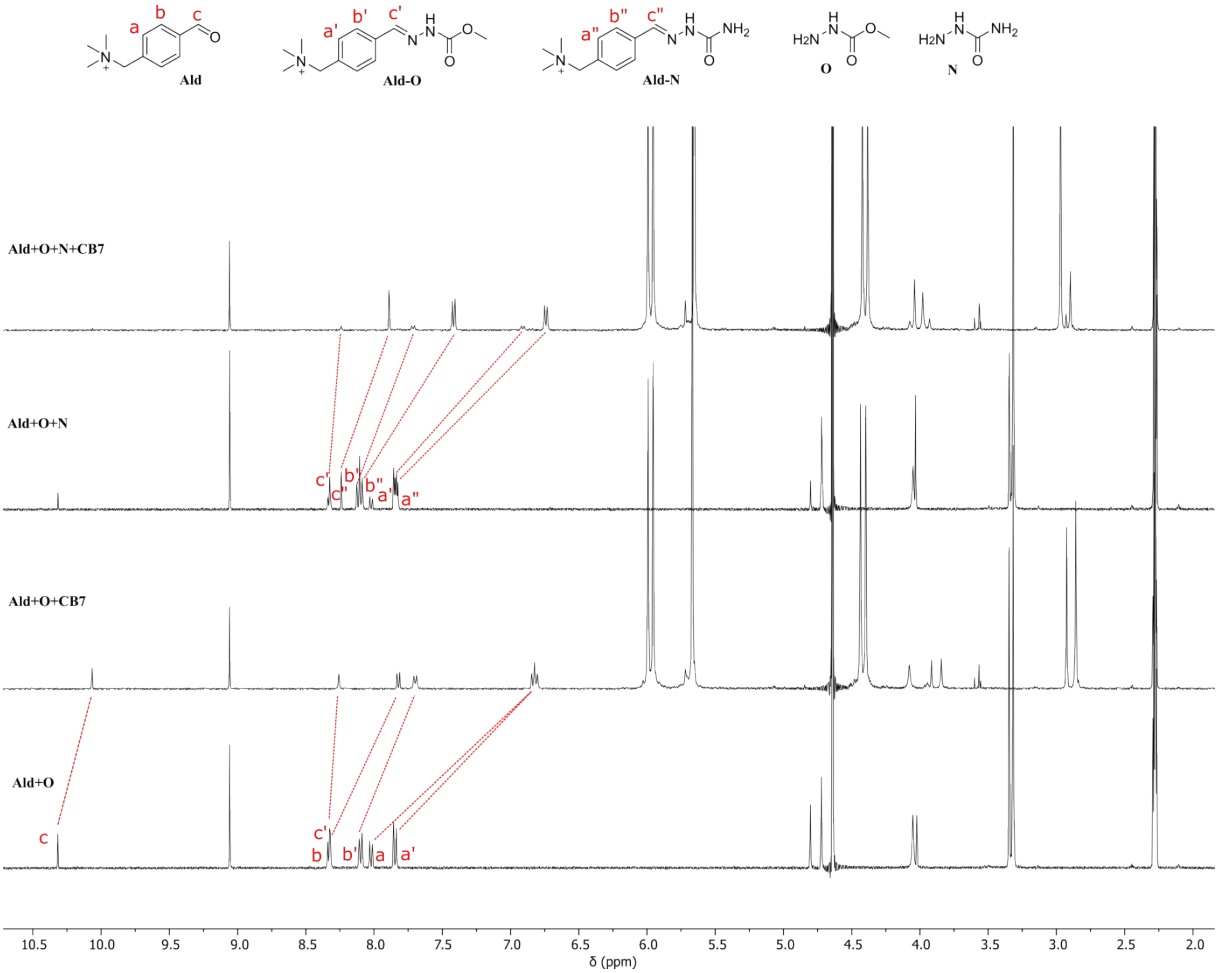

Figure S46. ^{1}H NMR spectra of Ald compound (1 equiv.), which emulates the benzaldehyde station in the pseudorotaxane, with methyl hydrazinocarboxylate (0.75 equiv.) and in a mixture with semicarbazide (0.75 equiv.) in the absence and presence of CB7 (1 equiv.) in MeCN-d_3/D_2O at 298 K. Based on more pronounced upfield shifts of a", b" and c" compared to a', b' and c', it can be concluded that CB7 ring in the complex with Ald-N product is closer to hydrazone residue than in the complex with Ald-O product, indicating some additional interaction between them.

Table S5. Distribution of substrates and products (mol %) in the reaction mixtures in the absence and presence of CB7. Note that Ald-f stands for unreacted Ald compound.

	Ald-f	Ald-O	Ald-N
Ald+O	39	61	-
Ald+O+CB7	39	61	-
Ald+O+N	15	38	47
Ald+O+N+CB7	3	19	78